4

Stability

4.1 Introduction

Hovercraft are rather different from conventional ships in that they operate in various modes:

- Floating on their hull like a boat;
- on cushion as a displacement craft below 'hump' speed;
- planing on the water surface above hump speed;
- running on various solid terrain conditions including ground, ice, snow, swamp, etc.

Additionally, the transition between modes 2 and 3 creates significant trim and may exert dynamic loads on the skirt system which make the craft less stable. Safe operation in waves while in mode 3 also requires attention to the influence of skirts on craft stability, particularly while the craft is travelling sideways or down-wave (or both at once!) at speed. Some of these manœuvres are unique to the ACV. Hovercraft stability changes in each of the different operating modes.

In chapter 1, we illustrated the limited stability of early craft, which led to a number of hovercraft overturning. Three British ACV overturned in April, May and July 1965 in Norway, the USA and England respectively. An American prototype SES, the XR.1 test craft, also overturned during trials and the Chinese air cushion craft 711 also overturned in Din Sah lake close to Shanghai during trials. An even more serious event happened to the Hovertravel passenger hovercraft, SR.N6–012, operating on the Solent between Portsmouth and Ryde in the Isle of Wight in March 1972. This overturned as a result of the combined action of both wind and waves in a sudden storm, with the deaths of five passengers (see section 4.7).

These accidents showed that the problems of dynamic instability are very complex and may result not only from unsatisfactory transient stability, but also poor course stability and the combined action of both wind and waves.

In this chapter we will investigate many problems which might lead to the capsizing of hovercraft due to dynamic instability and review the following analyses which form part of a typical ACV design:

- Stability of an SES hovering statically or travelling on a cushion;
- stability of an ACV hovering statically or travelling on a cushion;

- course stability and plough-in of ACVs running at high speed on calm water;
- longitudinal stability of an SES running at high speed in following waves – the broaching problem.

Owing to possible serious damage to structures, skirt, equipment and injury to passengers, or even capsizing of craft due to plough-in, the dynamic stability of an ACV and SES has been an important research topic for a number of years. Evaluation of the transient stability of an ACV/SES during take-off through hump speed and of the transverse stability of the craft in wind and waves has not yet been solved analytically due to the complicated nature of the response. Some work has been done and theoretical papers published, but at present the primary tools available to the designer are full scale trials of craft and their interpolation to new designs.

The criteria, standards, and rules of stability of an ACV/SES will be studied in Chapter 10, as they form a natural part of the design process. Most of these standards have been developed from the research, both analysis and testing, which is described in this chapter.

What is acceptable stability?

A hovercraft or SES requires a minimum positive stability moment arm in roll and pitch while floating or hovering statically and while moving. While moving, there should also be stability in yaw and sufficient moment to stabilize unsteady dynamic forces. Some simple rules may be given for guidance:

Static stability
Pitch: $h/L_c > 0.05p_c$ (metres)
Roll: $h/B_c > 0.08p_c$

Dynamic stability
Pitch: $h/L_c > 0.05p_c$
Roll: $h/B_c > 0.08p_c$
Yaw: $h/L_c > 0.02p_c$

Note: p_c is measured in metres of water head. Dynamic stability is measured at craft designed speed.

4.2 Static transverse stability of SES on cushion

Calculation of static transverse stability of an SES off cushion is similar to that for a conventional catamaran, so we can solve the problem for an SES by extending the calculation method for catamarans. As shown in Fig. 4.1, the air cushion force ($p_c.S_c$) will make a heeling moment with craft weight W, and the buoyancy of both sidewalls (γv_1, γv_2) will create a restoring moment.

This can be seen more clearly in the case of large heeling angle as shown in Fig. 4.2. While the heeling angle is zero, the cushion pressure is p_{c0} and when the heeling angle is θ, the cushion pressure becomes $p_{c\theta}$, which produce together with the craft weight a heeling moment, and the buoyancy caused by immersed section of the sidewalls produce a restoring moment.

The air leaks from under the left sidewall to cause a drifting motion. For this reason, the stability of an SES cushion is related not only to the thickness and

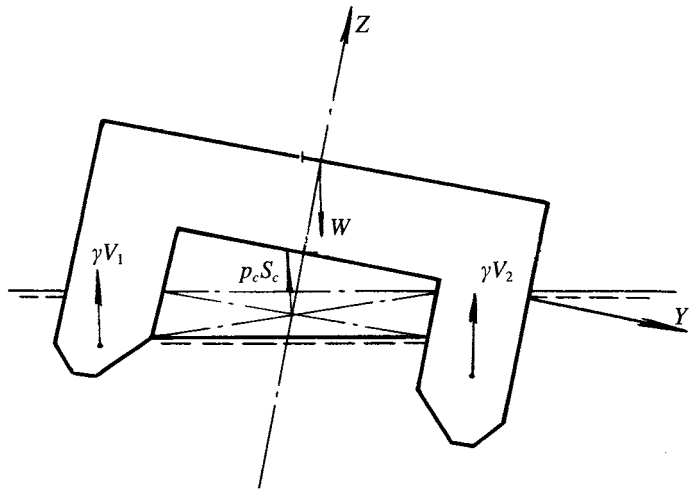

Fig. 4.1 Forces acting on SES due to heeling (sidewall emergence has not occurred).

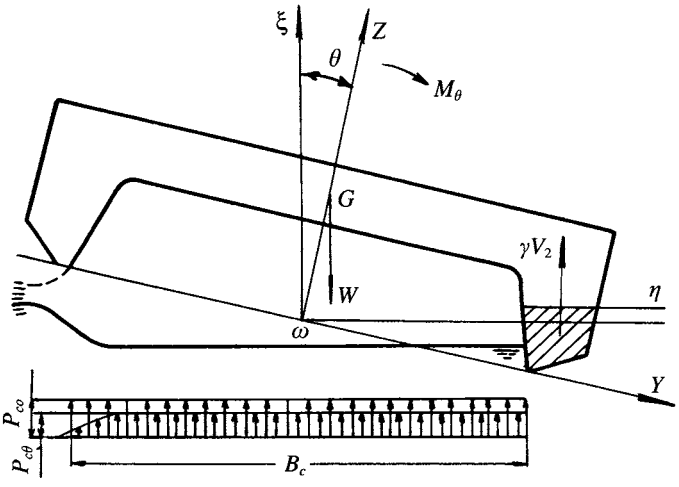

Fig. 4.2 Forces acting on SES due to heeling (one of the sidewalls has emerged).

displaced volume of the sidewalls, but also to the cushion pressure, air flow, gap height, vertical CG and bow/stern seal clearance.

Transverse stability on the US SES XR-1 decreased so severely during trials that it overturned while turning at high speed. This was caused by a combination of adoption of thin sidewalls to decrease water friction drag and the relative positions of the craft's longitudinal and vertical CGs.

In China, there has also been such experience. Poor transverse stability was experienced on the SES model 711–3 with thin sidewalls, the craft weight was increased from 1.825 to 2.2 t and the cushion pressure–length ratio from 19 to 24 kgf/m^3. The transverse stability decreased to an unacceptable degree so that

the ship rolled violently and periodically at low frequency, causing problems of control for the crews during sea trials.

It became clear that bow and stern skirt clearance needed to be altered to improve the transverse stability. However, over a long period of time, designers in China did not dare to remove the longitudinal stability keel (LSK), which was mounted in order to compartmentalize the cushion to improve the transverse stability, even though this gave a penalty of added drag and weight. Designers for a long time lacked the analytical and calculation methods to accurately predict transverse stability on cushion and so took the safe option, installing the LSK.

In order to estimate the transverse stability of an SES at the preliminary design phase, the graph in Fig. 4.3, showing the relation between transverse stability of craft on cushion and key craft geometrical parameters, may be used to ensure satisfactory stability. The figure shows that a satisfactory ratio of transverse metacentric height to cushion beam h/B_c can be obtained as soon as the relative thickness of sidewalls meets the relations shown in Fig. 4.3 for the cushion length/beam ratio (l_c/B_c) and pressure coefficient $p_c/(\sqrt[3]{D})$ (where D denotes the volumetric displacement of the craft and p_c cushion pressure) [40]. Figure 4.4 shows that the relation between the relative thickness of sidewall and cushion length/beam ratio. The shaded zone, represents the craft parameters with satisfactory transverse stability [19]. The figure was plotted by Kolezaev from statistical data obtained from practical ships. The figures are given for designer's reference as a starting point.

These two figures were made for reference at preliminary design. But since design norms have led to the change of some parameters, some craft have satisfactory transverse stability even though they do not comply with the requirements suggested by the two figures. Because these craft have other different parameters, such as different geometric

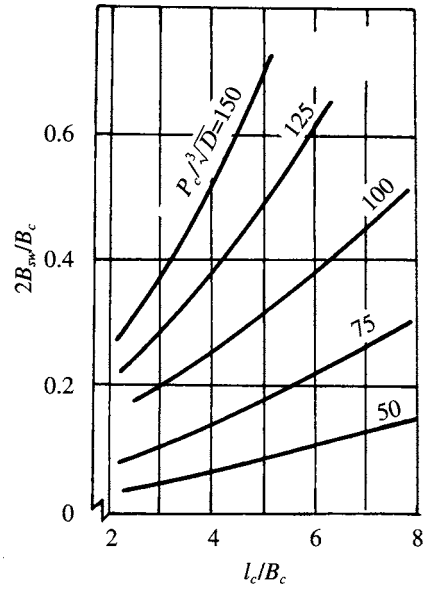

Fig. 4.3 Relation between relative sidewall thickness $2B_{sw}/B_c$ and L_c/B_c as well as equivalent cushion pressure length ratio $P_c/D^{0.33}$ (where D is the volumetric displacement of the craft).

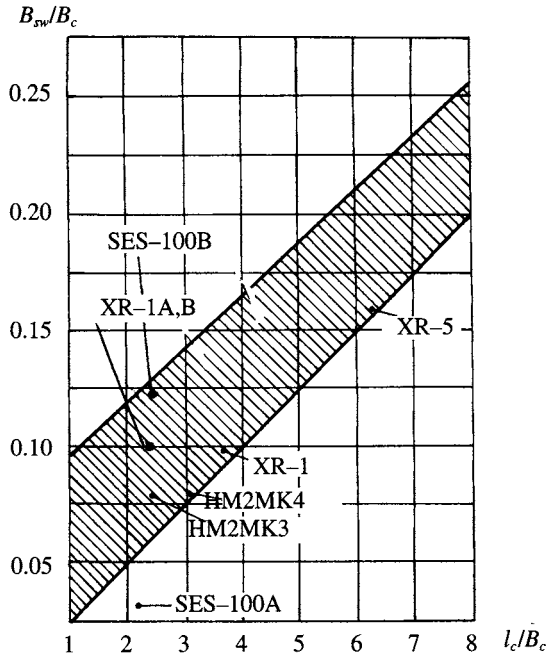

Fig. 4.4 Craft statistics of relative sidewall thickness and cushion length/beam ratio.

configuration of sidewalls, characteristic parameters of lift fans, and bow/stern seal clearance, one has to keep in mind that the various craft design parameters have to be similar to that adopted in the foregoing literature and the data cannot be used blindly.

For this reason, a number of complementary methods of calculating the transverse stability of an SES on cushion may be used to analyse the stability of the craft and understand the effect of various parameters on transverse stability.

Calculation method for predicting SES static transverse stability on cushion [41]

We introduce here a calculation method for predicting the static transverse stability of SES without LSK on cushion. The method for the SES with longitudinal keel can also be obtained by similar deduction, but it is not necessary to introduce the latter because no LSKs are mounted on modern SES.

The general assumptions for the calculation method are as follows:

1. The cushion pressure is distributed uniformly in the plenum chamber of the craft in the case of either upright condition or heeling.
2. One may presume that the drifting force caused by the difference of the leakage air momentum under both sidewalls of a heeling craft is equal to the lateral hydrodynamic force acting on them and the heeling moment caused by this induced couple may be neglected.
3. The fan outlet is perpendicular to the wet deck of the craft and the total fan flow blows directly into the plenum chamber.

4. The gaps between the lower edge of both bow and stern seals and the base-line are equal.

Calculation of static transverse stability for an SES without LSK

The typical midship transverse section of an SES and the forces acting on it are shown in Fig. 4.5. First of all, we can determine the equilibrium water line of the craft in the case of heeling, which is very similar to the method for predicting the running attitude of craft introduced in Chapter 5. The method is based on the equations of weight, flow continuity, fan characteristic and energy. Then the resulting moment at the given heeling angle can be obtained according to the equilibrium water-line.

1. Energy equation:

$$H_j = P_c + 0.5\rho_a \xi (Q/S_o)^2 \tag{4.1}$$

where H_j is the total pressure of the fan (N/m^2), P_c the cushion pressure (N/m^2), ξ the coefficient due to the pressure loss, Q the flow rate (m^3/s) and S_o the area of outlet of the air duct (m^2).

2. Flow continuity equation:

$$Q = Q_{sb} + Q_{sw} \tag{4.2}$$

$$Q_{sb} = Q_s + Q_b \tag{4.3}$$

$$Q = Q_s + Q_b + Q_{sw} \tag{4.4}$$

where Q_s is the air leakage from under the stern seal (m^3/s), Q_b the air leakage due to bow trim (m^3/s), and Q_{sw} is the air leakage under the sidewalls.

3. Flow rate equation:
Air leakage flow under the bow/stern seals can be written as

$$Q_s = Q_b = K\phi A_{j1}\sqrt{2p_c/\rho_a} \tag{4.5}$$

where K is the correction coefficient due to the effect of water surface, ϕ the flow coefficient and A_{j1} air leakage area under the bow and stern seals (m^2) (they are a function of inner draft t and craft trim angle).

The flow under the sidewalls can be written as

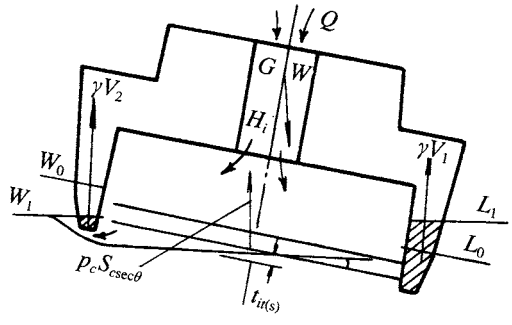

Fig. 4.5 Typical forces acting on skirt heeling craft.

$$Q_{sw} = K\phi A_{j2}\sqrt{2p_c/\rho_a} \tag{4.6}$$

where A_{j2} is the leakage area under sidewalls (m^2) (they are a function of inner draft t_i and heeling angle θ).

4. Fan characteristic equation:

$$H_j = A + BQ + CQ^2 \tag{4.7}$$

where A, B, C are fan characteristic coefficients which can be obtained according to the type, speed, etc.

5. Weight equilibrium equation:

$$W = p_c S_c \cos\theta + \gamma (V_1 + V_2) \tag{4.8}$$

where S_c is the cushion area (m^2), γ the specific weight (N/m^3), V_1 the volumetric displacement of the immersed sidewalls (m^3), V_2 the volumetric displacement of the emerged sidewalls (m^3) and W the craft weight (N).

Substitute equations (4.1)–(4.6) into equation (4.7), then we have

$$[1 + (2A_{j1} + A_{j2})^2 k^2\phi^2/S_0^2 - 2C/\rho_a(2A_{j1} + A_{j2})^2 k^2\phi^2]p_c - B(A_{j1} + A_{j2})k\phi(2p_c/\rho_a) - A = 0 \tag{4.9}$$

Equation (4.9) only includes p_c and air leakage area A_{j1}, A_{j2} which are only related to inner draft t_i and heeling angle θ. Therefore by combining the two equations (4.8) and (4.9), the p_c and t_{i0} at different θ can be solved by iteration with the aid of a computer.

This method is similar to that used on conventional ships, i.e. determining the equilibrium water line at the heeling condition, then the buoyancy of the sidewalls and cushion pressure can be easily obtained; the difference is that the weight of the craft must equal the sum of cushion lift and buoyancy provided by the sidewalls and the cushion pressure has to satisfy the fan characteristic equation, flow equation and energy equation.

Based on the equilibrium water line, the righting moment can be obtained as follows:

$$M_\theta = (l_{m1}V_1 - l_{m2}V_2)\gamma - (\overline{KG} - t_{im})W\sin\theta \tag{4.10}$$

where M_θ is the righting moment of the craft at the heeling angle (Nm), l_{m1} the transverse distance between the centre of buoyancy of γV_1 and CG of the craft (m), l_{m2} the transverse distance between the centre of buoyancy of γV_2 and CG of the craft (m) at any given heeling angle and $\overline{KG}$ the height of the centre of gravity above the keel.

6. A block diagram for the calculation can be seen in Fig. 4.6.

Model and full-scale tests for static transverse stability of an SES on cushion

Measurements of hovercraft static trim and heel can be made directly from a scale model, or a full-scale craft. The trim or heel can be related to known shifts of weight and therefore turning moment. Such data may be plotted against theoretical calculations such as that described in 4.2 to verify the analysis, or allow empirical adjustment to it. An example is described below, from MARIC experience.

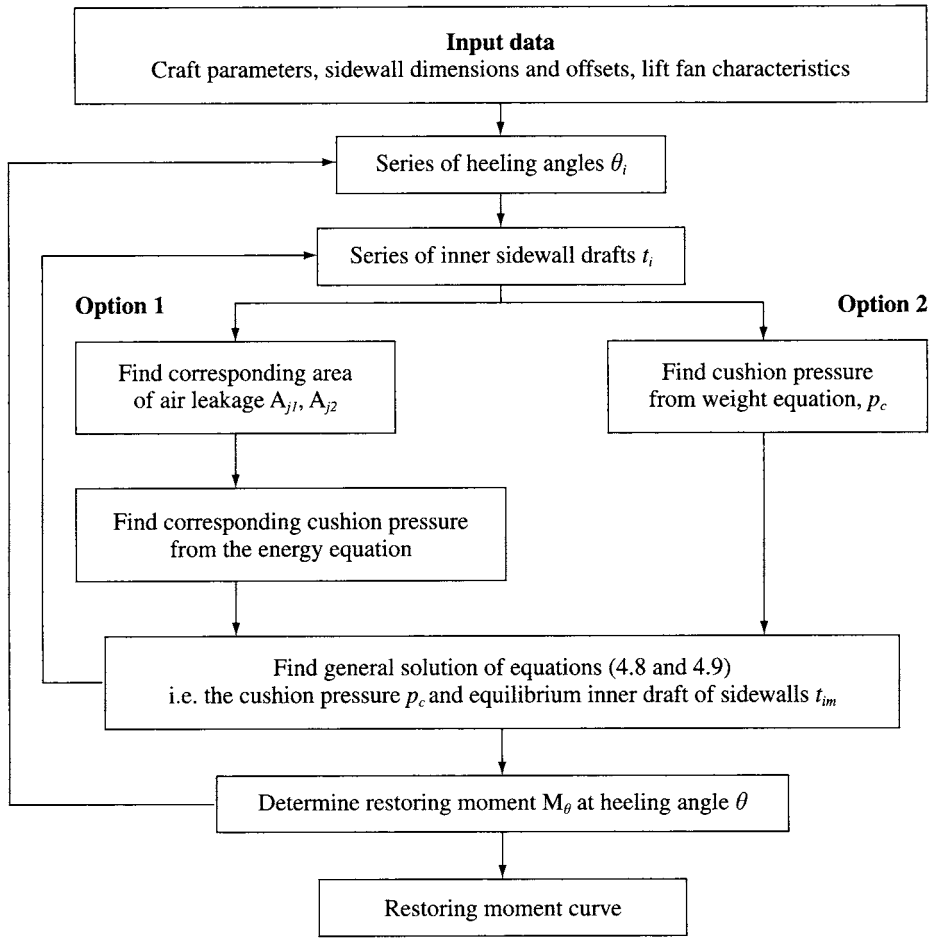

Fig. 4.6 Block diagram for calculating the static transverse stability of SES on cushion.

Model and test facility

The static transverse stability for two SES models on cushion were determined by direct measurements at MARIC and dynamic transverse stability tests were also carried out for one of these models.

The leading particulars for both models are shown in Table 4.1 and a typical section of the sidewall is shown in Fig. 4.7. During the tests, solid ballast was moved to cause model heeling, then the heeling angle measured by a clinometer.

Experimental results

During heeling of an SES on cushion, the restoring moment of the craft will be due mainly to the difference in buoyancy of the sidewalls unless the sidewalls are very thin. Experiments normally include the following:

1. Determining the effect of the fan speed on the static transverse stability.

Table 4.1 The leading particulars of two craft models

Name	Units	Nomenclature	Model No. 1	Model No. 2
Cushion length	m	l	1.61	2
Cushion beam	m	B_c	0.35	0.492
Height of sidewalls	m	h_s	0.056	0.167
Height of hard chine	m	h_k	0.042	0.067
Width of sidewalls	m	B_{sw}	0.05	0.067
Width of sidewall keel	m	B_1	0.015	0.025
Sidewall deadrise angle	deg	a	65	75
Flare angle of sidewall above hard chine	deg	β	89	90
All-up weight	N	W	156	406
Cushion pressure	N/m^2	p_c	290 approx.	370 approx.

2. Determining the effect of the longitudinal stability keel on the static transverse stability if this is fitted. This can be achieved by blocking the delivery duct to the stability keel on the model or full-scale craft to stop it inflating.

The effect of fan speed of the models on transverse stability is shown in Figs 4.8 and 4.9.

Similar experiments may be carried out for trim (longitudinal stability). In this case, the sidewall buoyancy has greater effect trimming bow up than bow down, due to the finer bow form.

Effect of various parameters on transverse stability

It is not practical to study the effect of all the various parameters by testing because of the amount of work involved. Therefore the research method at MARIC has been to gather sufficient data to verify the foregoing calculation method with aid of model experiments. We can discuss the effect of some of the remaining parameters on the transverse stability by using the calculation methods.

Effect of sidewall geometric configuration on the static transverse stability

Taking the SES model 717 as an example, we calculate the static transverse stability of the craft with a specific fan speed, duct configuration and form of the seals, and

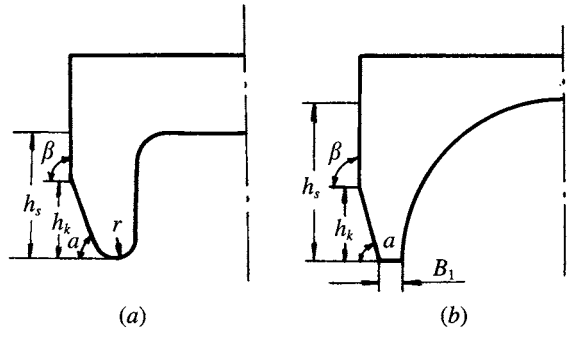

Fig. 4.7 Typical transverse section of two craft models with different inner sidewall geometries. (a) Model 1, (b) model 2.

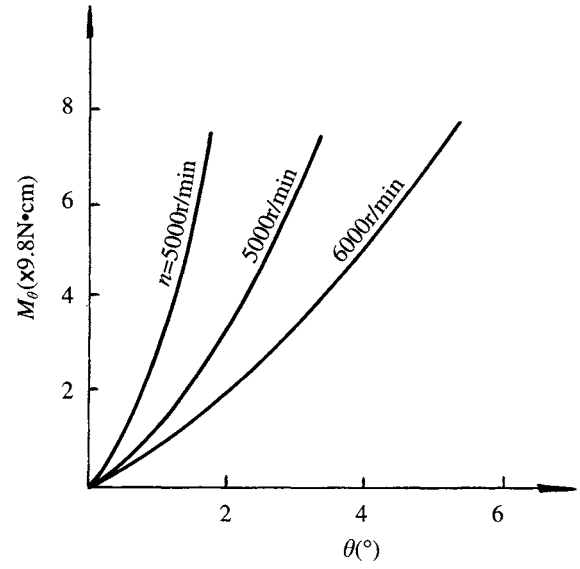

Fig. 4.8 Heeling restoring moment of model craft No. 1 with different fan speeds and heeling angles.

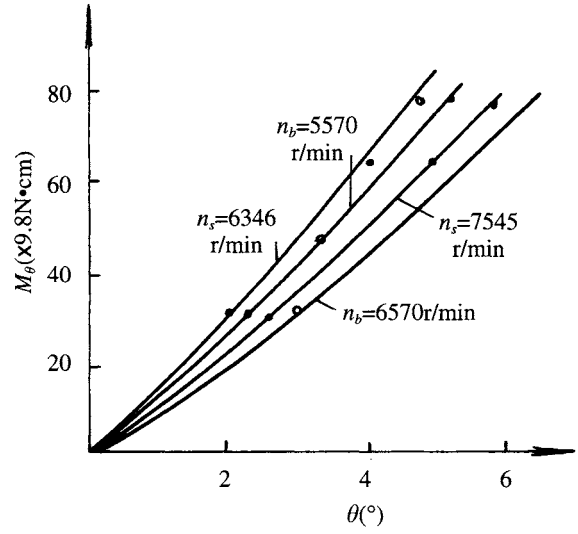

Fig. 4.9 Heeling restoring moment of model craft No. 2 with different fan speeds and heeling angles.

vary the geometric configurations of the sidewall amidships, in order to evaluate the effect of the geometric configuration of sidewalls on transverse stability.

The effect of the lines of a bow sidewall is smaller than that of midship lines. If we assume that the lines of the bow sidewall will be fixed and the line of hard chine is above the loaded water line, then the main parameters of the sidewall can be defined as follows:

1. width of keel plate of sidewall, B_1;
2. deadrise angle of midships section of sidewalls, a;
3. height of hard chine line amidships, h_k;
4. width of sidewall, B_{sw};
5. flare angle of sidewall above hard chine, β;
6. external draft of the sidewall, t_0.

From Fig. 4.10, we have

$$B_{sw} = B_1 + t_0 \cot a \tag{4.11}$$

$$B_{sw}/B_c = (B_1 + t_0 \cot a)/B_c \tag{4.12}$$

In general, B_1 can be kept as a constant, t_0 can be determined by the cushion pressure p_c, so we can take the parameters a, β and B_{sw} as variables, the variable range of which is shown in Table 4.2.

The calculation results are shown in Fig. 4.11. In order to investigate the effect of B_1 on stability, we obtain the second set of variables shown in Table 4.3. The basic parameters were kept the same as for craft type 717, such as principal dimensions, cushion pressure/length ratio, flow rate coefficient, flare angle of sidewall section above the hard chine, the gap between the lower edge of the bow/stern seals and the base-line, fan characteristic, etc., except the parameters a and β. Then the static transverse stability could be calculated. The results are as shown in Fig. 4.12.

From the figures, it is found that:

1. The static transverse stability of craft at large heeling angles is strongly affected, but not at small angles.

Table 4.2 The variable range of a, β, B_{sw}

a (°)	40	45	50	55	60
β (m)	55, 60, 65	50, 60, 65	60, 65, 70	60, 65, 70	65, 70
B_{sw}	0.62	0.54	0.472	0.414	0.362
B_{sw}/B_c	0.177	0.154	0.135	0.118	0.104

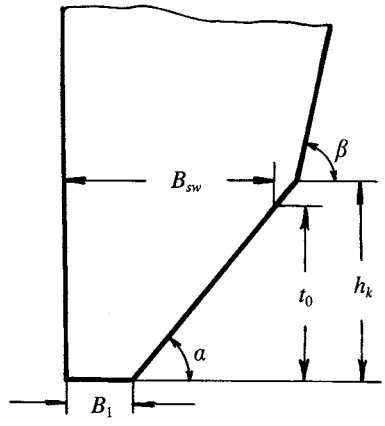

Fig. 4.10 Geometrical parameters for sidewalls.

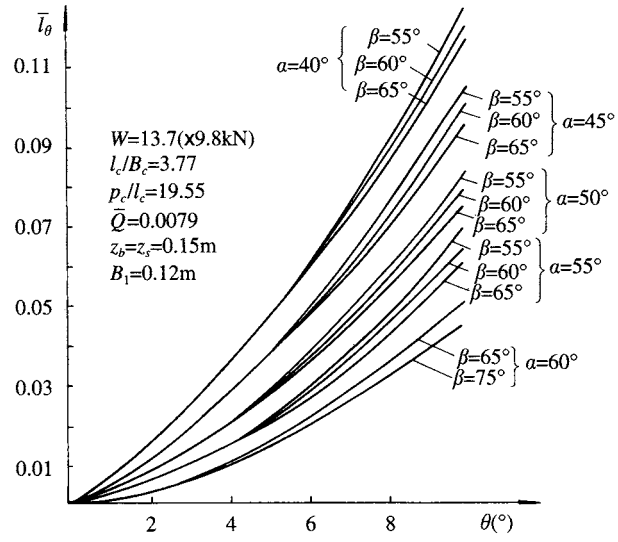

Fig. 4.11 Influence of parameters α, β on relative heeling righting arm.

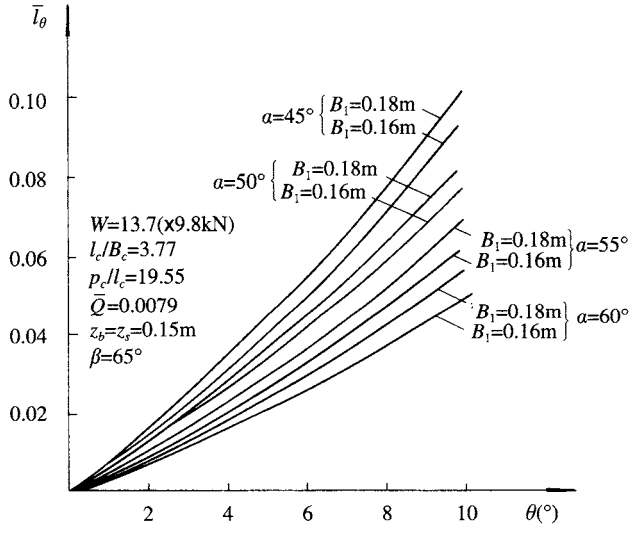

Fig. 4.12 Influence of parameters α, β on relative heeling righting arm.

2. Linearity in the relation of the righting arm with respect to the heeling angle only exists at small heeling angles to about 3–4°, therefore it is convenient to take the relative metacentric height $\bar{h} = h/B_c$, where h is the metacentric height and B_c is the cushion beam, as one of the stability criteria of the craft.
3. The width of the keel plate on the sidewall does not strongly affect the stability either at small heeling angles or at large angles.
4. α strongly affects the stability at both small or large heeling angles.

Table 4.3 The variable range of a, B

a (°)	45	45	50	50	55	55	60	60	60
B (m)	0.16	0.18	0.16	0.18	0.16	0.18	0.16	0.18	0.20
B_{sw}/B_c	0.166	0.171	0.146	0.152	0.13	0.135	0.115	0.121	0.126

5. According to the two sets of variables mentioned above, we can obtain the relation of the relative metacentric height $\bar{h}$ with respect to the relative thickness of the sidewall, B_{sw}/B_c (Fig. 4.13). It is found that this relation is stable whatever set of variables are used to obtain the values of B_{sw}/B_c. Therefore, it is convenient to take the relative thickness of the sidewall B_{sw}/B_c as a main parameter assumed to control transverse stability, at the preliminary design stage.

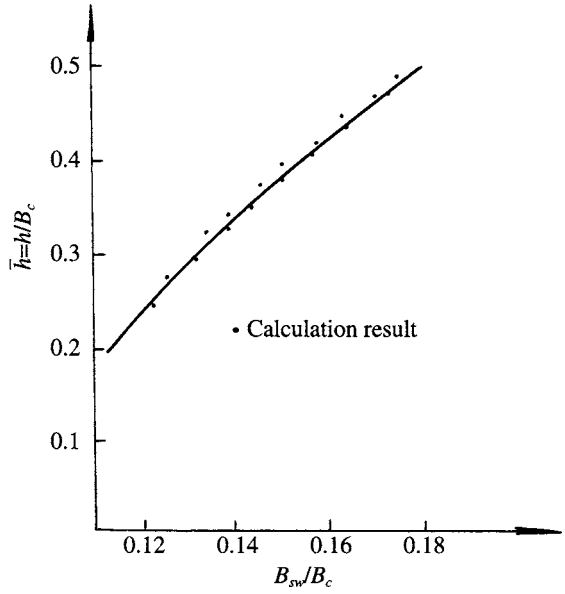

Fig. 4.13 Relative sidewall thickness B_{sw}/B_c and relative initial static transverse metacentric height.

Effect of the lift power (or the fan speed) on the transverse stability

In the calculation equations we can see that the fan flow rate strongly affects the stability. In general the static transverse stability deteriorates as the fan flow rate increases. It seems that the stability of a craft on cushion is worse than that off cushion, because the cushion pressure causes a negative transverse stability.

Figure 4.14 shows the effect of the relative flow coefficient $\bar{Q}$ on the relative metacentric height $\bar{h}$. For example, $\bar{h}$ decreases from 0.163 to 0.135 when $\bar{Q}$ increases from 0.006 15 to 0.008 92 (i.e. fan speed increases from 1300 to 1600 rpm).

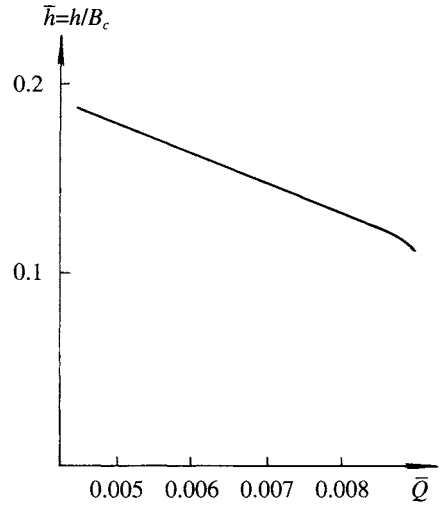

Fig. 4.14 Variation of relative initial static transverse metacentric height with air flow rate coefficient $\bar{Q}$.

Effect of the cushion pressure length ratio (p_c/l_c) on the transverse stability

The calculated results of stability with various cushion pressure/length ratios are shown in Fig. 4.15. It is found that the relative metacentric height $\bar{h}$ decreases from 0.133 to 0.123 when the cushion pressure/length ratio increases from 21.47 to 23.06 kgf/m^2.

Effect of the gap between the lower edge of bow/stern seals and the base-line

To make a simple calculation of the transverse stability, at MARIC we assumed the gaps between the base-line and the lower edge of bow/stern seals to be the same, to calculate the transverse stability of craft type 711–3 with various inner drafts of the sidewalls, $z_{b,s}$, by running the fan at different speeds.

The calculated results are shown in Fig. 4.16. Transverse stability increases with the inner draft of the sidewalls, though the benefit is not greater than that obtained by increasing the thickness of the sidewalls. This means that adjustment of the draft of the sidewall is a good way to control transverse stability of a craft in operation.

This phenomenon can be traced back to the trials of craft type 717-III in 1969. At the beginning, the craft operated quite well with satisfactory speed and transverse stability. After some modifications, the all-up weight of the craft increased from 1.8 to 2.2 t, and the cushion pressure/length ratio increased from 19 to 24 kgf/m^3 and it was discovered that the transverse stability of the craft had deteriorated. The craft used to roll slowly with a rolling angle up to 12° even in ripples. After increasing the inner draft of the sidewall at the stern from 0.24 to 0.28 m the unstable rolling disappeared.

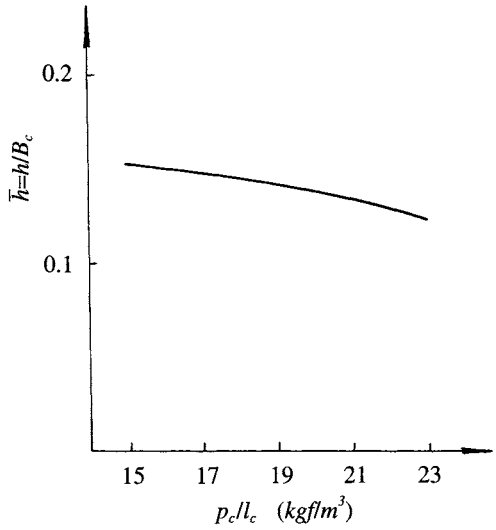

Fig. 4.15 Relative transverse righting arm l_θ variation with cushion length beam ratio P_c/L_c.

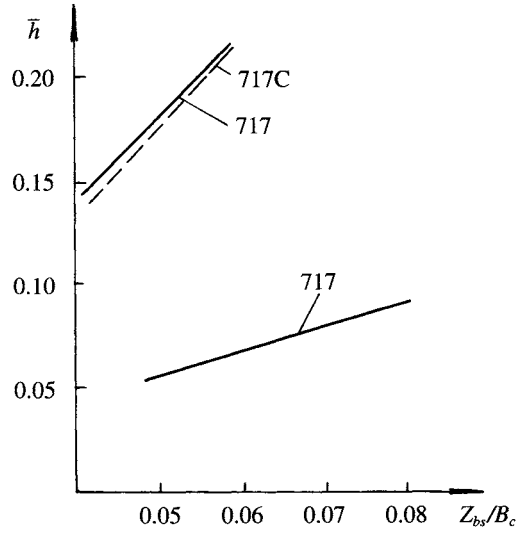

Fig. 4.16 Influence of bow/stern seal relative gap $Z_{b,s}/B_c$ on relative initial static transverse metacentric height.

Effect of the cushion length beam ratio on the transverse stability

The calculated transverse stability of craft type 717 with different cushion length/beam ratios is shown in Fig. 4.17.

From Table 4.4, it is found that the initial transverse stability at large heeling angles will not change significantly, for several variations of SES type 717, as long as the cushion pressure is kept constant, even though with different cushion length/beam ratio, weight and cushion pressure/length ratio for different types of craft. It is not

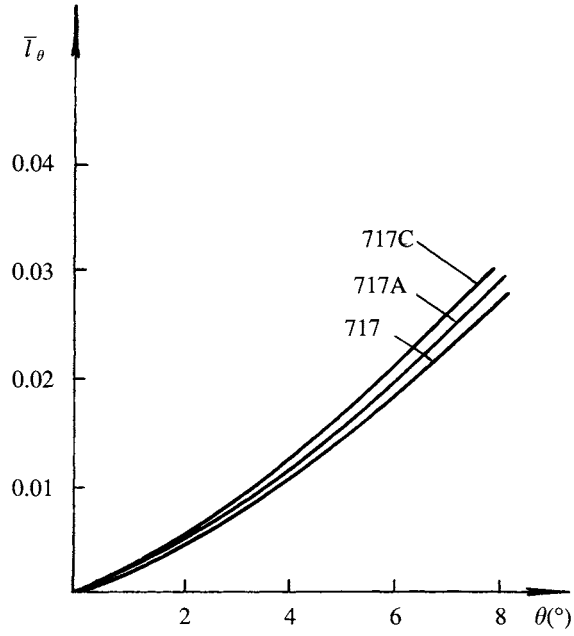

Fig. 4.17 Static transverse stability for three craft of series 717.

Table 4.4 The leading particulars for three SES type 717

Item	Symbols	Dimensions	717	717A	717C
Craft weight	W	t	13.7	15.95	18.20
Cushion length	l_c	m	13.2	15.2	17.3
Cushion beam	B_c	m	3.5	3.5	3.5
Cushion l/b ratio	l_c/B_c		3.77	4.34	4.94
Cushion pressure length ratio	p_c/l_c	kgf/m^3	19.93	17.31	15.38
Cushion pressure	p_c	N/m^2	2630	2630	2660
Flow coefficient	Q		0.00757	0.00658	0.00570
VCG	KG	m	1.27	1.27	1.27
Bow and stern seals clearance	$z_{b,s}$	m	0.15	0.15	0.15
Sidewall midship deadrise angle	α	deg	60	60	60
Sidewall flare above hard chine	β	deg	89	89	89
Sidewall keel plate width	B_1	m	0.12	0.12	0.12

correct, therefore, to say that the transverse stability will definitely deteriorate with increasing cushion length/beam ratio; one has to analyse the particular craft design to identify its sensitivity to this possible problem.

Summary

1. The calculated results of the static transverse stability of craft by means of this method agree well with the experimental results, therefore it can be recommended to use this method to check and analyse the static transverse stability of the designed or constructed SES.

2. The relative thickness of the sidewall might be considered as a main parameter that will strongly affect the transverse stability of craft.
3. The transverse stability of constructed craft can be improved by decreasing the flow rate coefficient ($\bar{Q}$), cushion pressure/length ratio (p_c/l_c) and by increasing the sidewall draft under the bow/stern seals ($z_{b,s}$).
4. Increasing cushion length/beam ratio might occasionally result in a deterioration of the transverse stability, but it might not be the only result since so many factors are involved. It is best to carry out a parametric sensitivity analysis of stability to make a first assessment and if possible follow up with model tests, if the geometry is significantly changed from the base case.

Approximate calculation of SES static transverse stability on cushion

At the preliminary design stage, computer methods (apart from spreadsheet calculations) cannot be adopted because the offsets and some main parameters of the craft are lacking. Therefore the following relationship deduced from experimental results from Hovermarine SES craft [42] can help:

$$h = \gamma A_s (B_c + A_s/L_s)^2 / 2W - \gamma S_c p_c / W + [0.5 L_s \tan \tau + p_c] - \overline{KG} \qquad (4.13)$$

where h is the initial transverse metacentric height of craft (alternately GM) (m), γ the mass density of water (N/m^3), A_s the water-plane area of one sidewall at hovering water-line excluding internal bulges (m^3), B_c the cushion beam of craft at water-line (m), L_s the sidewall length (m), τ the static trim angle (°), p_c the cushion pressure head (m H_2O), S_c the cushion area (m^2), KG the height of centre of gravity (m) and W the mass of craft (N).

This expression assumes a small angle of heel with no loss of cushion pressure. In practice it is suitable for estimation up to an angle of $\tan^{-1}(p_c/B)$, i.e. typically 3–5° heel. It is also significantly affected by craft trim and cushion air flow. Blyth [42] has carried out a substantial model test programme to investigate the dynamic stability of SES of differing geometries in a seaway; this has been the basis for stability criteria adopted by the IMO. The recommendations are presented following the description of similar investigations carried out by MARIC below.

4.3 SES transverse dynamic stability

SES often run at high speed, so the forces acting on an SES during heeling are rather different from the static situation. It is therefore very important to investigate the transverse stability of an SES on cushion in order to develop appropriate calculation methods by which the effect of speed and various geometrical parameters can be determined.

We will introduce a method for calculating the dynamic transverse stability of craft in this section. First of all we have to determine the craft trim at speed, then define the righting moment of the craft in motion during the heeling situation.

Calculation of craft trim

According to the method in Chapter 5, we can determine the craft trim at various speeds based on four relationships from equation (5.12) and the other two equations (5.13, 5.14) due to the deformation of the water surface caused by wave-making of the craft. This method is rather complicated, especially for the calculation of deformation of the water surface. We recommend the use of a simplified method for estimating craft trim and for calculating the forces acting on the craft as follows:

1. In the case of a craft with bag and finger type skirt, the lift of skirt can be calculated as

$$\left.\begin{array}{ll} \text{when } (z_b - t_{bi}) \geqslant 0 & L_{bs} = 0 \\ \text{when } (z_b - t_{bi}) < 0 & L_{bs} = P_c S_c l(z_b - t_{bi})|\cos(a_b) \end{array}\right\} \tag{4.14}$$

   where L_{bs} is the lift due to the bow skirt with bag and finger type, z_b the gap between lower tip of bow finger and sidewall base-line (m), t_{bi} the inner draft of sidewalls at bow (m), and a_b the declination angle of bow fingers with horizontal plane, as shown in Fig. 4.18 (°).
2. In the case of using a planing plate as the stern seal, the planing plate can be calculated by the theory of Chekhof [43], i.e. as a two-dimensional planing plate running in gravitational flow, and estimate the lift as follows:

$$\left.\begin{array}{ll} \text{when } (z_s - t_{si}) \geqslant 0 & L_{ss} = 0 \\ \text{when } (z_s - t_{si}) < 0 & L_{ss} = 0.5\pi\rho_w v^2 l B_c a_s[l - Fr_l^{-2}(\pi^2 + 4)/2\pi] \end{array}\right\} \tag{4.15}$$

   where z_s is the gap between the lower tip of the stern seal and base-line (m), t_{si} the inner draft of sidewall at stern (m), v the craft speed (m/s), L_{ss} the lift acting on planing plate (N), l the length of wetted plate (m), a_s the angle of attack (°) (here we assume the trim angle is zero, therefore the angle of attack is equal to the angle between the plate and flow direction).

   Since the wetted length is small and Fr is large, the calculation can also be simplified to a two-dimensional plate in non-gravitational flow as follows:

$$L_{ss} = 0.5\pi\rho_w v^2 l B_c a_s \tag{4.16}$$

3. In the case of stern seals of the double bag type (Fig. 4.19(b)), the lift acting on the skirt can be calculated as

$$\left.\begin{array}{ll} \text{when } (z_s - t_{si}) \geqslant 0 & L_{ss} = 0 \\ \text{when } (z_s - t_{si}) < 0 & L_{ss} = p_c B_c l t_{si} - z_s|\text{cosec } a_s \end{array}\right\} \tag{4.17}$$

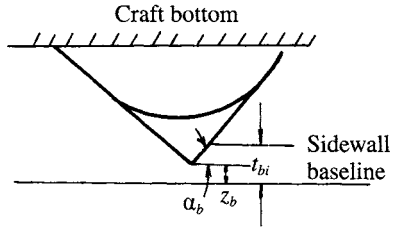

Fig. 4.18 Configuration of bag and finger type bow skirt.

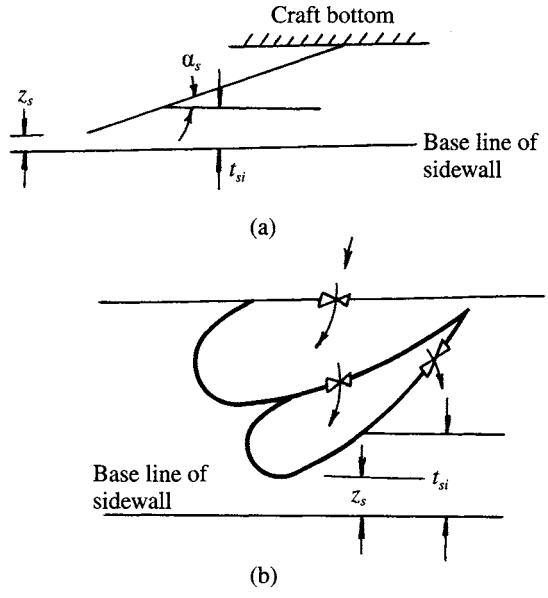

Fig. 4.19 Geometry of stern seals: (a) planing stern seal; (b) twin bag skirt.

where L_{ss} is the lift acting on the stern skirt (N) and a_s the declination angle between the lower base-line of stern seal and sidewalls (°). The calculation is also similar for triple-bag SES stern skirts.

4. Two simplified added equations can be adopted from equation (3.12),

$$t_{bi} \approx t_{bo}$$
$$R_w \cong W(t_{os} - t_{is})/l_c \tag{3.12}$$

The wave-making drag R_w can be calculated by the methods described in Chapter 3, and then the running attitude of the craft may be obtained using the foregoing equations.

SES transverse stability on cushion in motion

It is not difficult to define the transverse stability moment and lever arm after determining the SES trim. Two conditions of the craft can be analysed as follows.

Calculation of transverse stability for the SES with flexible bow/stern seals

In the case of an SES with flexible bow/stern seal, it can be assumed that the restoring moment acting on the craft running on cushion and heeling is equal to the sum of the heeling moment caused by the air cushion and the restoring moment due to sidewalls and both bow/stern seals. Considering that the length/beam ratio of the sidewalls is very large, normally 34–50 in fact, the dynamic lift due to the sidewalls is very small and can be neglected, thus the restoring moment can be calculated as follows. When $(z_b - t_{bi}) > 0$

$$\Delta M = \int_{(z_b - t_{bi})\cot\theta}^{Bc/2} p_c[y\tan\theta - (z_b - t_{bi})]c_{sc}a_b y\mathrm{d}y$$
$$= 1/3\, p_c c_{sc} a_b \tan\theta\,[B_c^3/8 - (z_b - t_{bi})^3\cot^3\theta]$$
$$- 0.5\, p_c c_{sc} a_b (z_b - t_{bi})[B_c^2/4 - (z_b - t_{bi})^2\cot^2\theta] \quad (4.18)$$

where ΔM is the transverse restoring moment due to bow/stern skirts (N m) and y the abscissa of the craft (m) (Fig. 4.20).

The block diagram for predicting the craft trim in motion is as shown in Fig. 4.21.

Calculation of the transverse stability of SES with rigid stern seal

The foregoing calculation procedure cannot be used in the case of the rigid stern seal, because the lift acting on the planing plate is so much larger than that on the flexible skirts at same heeling angles, and leads to a trim moment to change the running attitude, cushion pressure and other parameters, etc. The changing running attitude may be obtained by means of an iteration method, from which the stern plate lift and restoring moment on the craft can then be determined.

Since the end of the planing plate is close to the craft sidewall when heeling it can be considered as a two-dimensional planing plate and the other end of the plate can be considered as a three-dimensional planing plate. The lift of whole plate can also be considered as the arithmetic mean of both two- and three-dimensional planing plates. The transverse restoring moment due to the stern plate can be written as

$$\Delta M = \int_{(z_s - t_{si})\cot\theta}^{B_c/2} (0.5\,\rho_w v^2 \pi a_s)[y\tan\theta - (z_s - t_{si})]c_{sc}a_s y\mathrm{d}y$$
$$= 1/3\,(0.5\,\rho_w v^2 \pi a_s)c_{sc}a_s\tan\theta\,[B_c^3/8 - (z_b - t_{bi})^3\cot^3\theta]$$
$$- 0.5\,(0.5\,\rho_w v^2 \pi a_s)c_{sc}a_b(z_s - t_{si})[B_c^2/4 - (z_s - t_{si})^2\cot^2\theta] \quad (4.19)$$

where ΔM is the restoring moment due to the stern plate of the craft at heeling (N m) and θ the heeling angle (°).

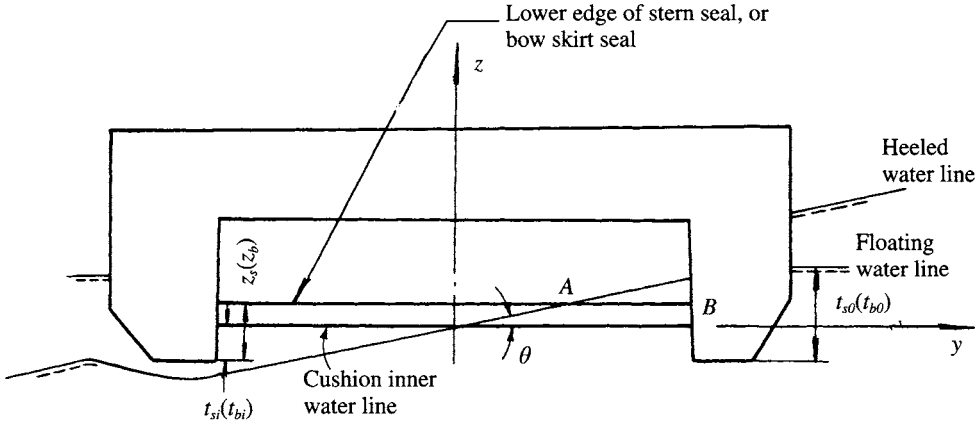

Fig. 4.20 Calculation for righting moment of bow/stern seal during heeling of craft.

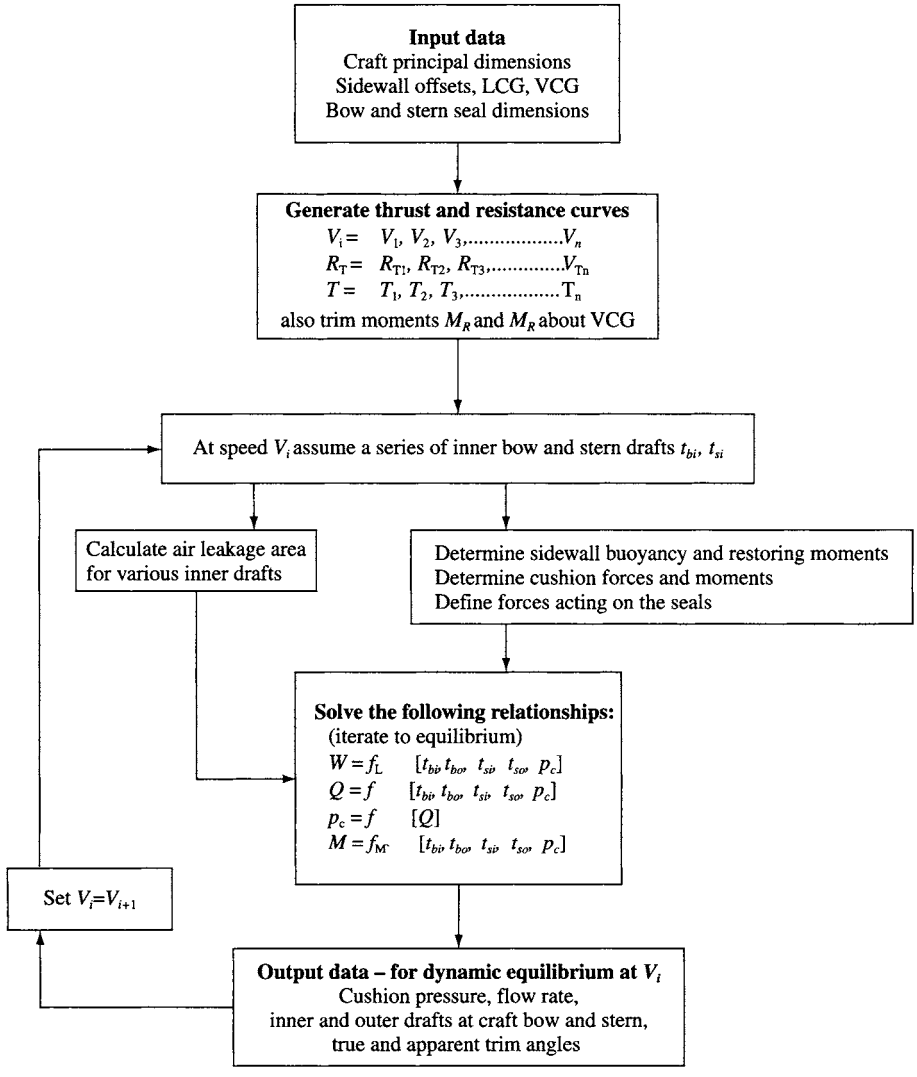

Fig. 4.21 Block diagram for calculating craft dynamic trim.

The block diagram for predicting the transverse stability of the craft at speed is shown in Fig. 4.22.

Calculation results for two actual craft

The calculation results for the SES types 717A and 717C using the foregoing method and computer analysis can be described as follows.

Calculation of running attitude of the craft (simplified method)

1. For SES type 717A (Table 4.5):

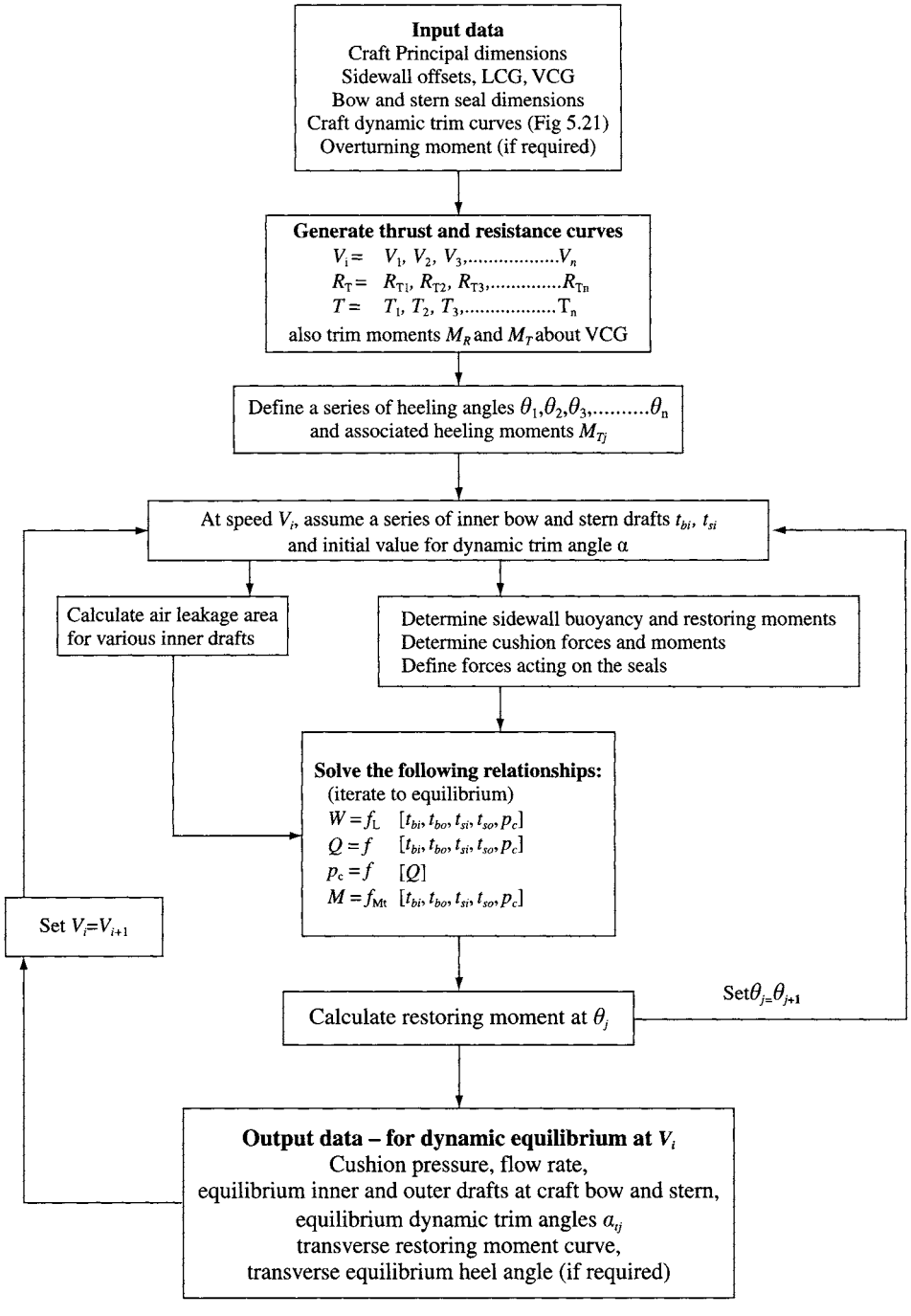

Fig. 4.22 Block diagram for calculating dynamic transverse stability.

Craft weight: $W = 156$ kN
Fan characteristics: $A = 631$
$B = -1.80$
$C = -0.187$
$S_i = 0.24\ m^2$

Principal dimensions and parameters of the craft:

$B_c = 3.5$ m
$B_{sw} = 0.13$ m
$B_{swb} = 0.06$ m (width of the sidewall at bow)
$H_{sw} = 0.43$ m (height of the sidewall)
$a_b = 70°$ (deadrise of sidewall at bow)
$a = 60°$ (deadrise of the sidewall amidships)
$S_a = 14\ m^2$ (frontal area of the superstructure)
$a_s = 9.23°$ (inclination between the stern plate and base-line)
$x_g = -0.20$ m (aft amidships)
$\overline{KG} = 1.22$ m
$H_s = 0.50$ m (height of thrust for water jet propulsion over base-line)

2. SES type 717C (Table 4.6):

Craft weight: $W = 156$ kN
Fan characteristics: $A = 631$
$B = -1.80$
$C = -0.187$
$S_i = 0.24\ m^2$

Table 4.5 The calculation of running attitude of the SES type 717A at various speeds

Item	Symbol	Units			
Craft speed	V	km/h	30.67	42.90	51.08
Cushion pressure	p_c	N/m^2	2690	2716	2763
Flow rate	Q	m^3/s	23.65	23.55	23.38
Outer draft at stern	T_{so}	m	0.402	0.386	0.356
Inner draft at stern	T_{si}	m	0.0389	0.0399	0.0517
Outer draft at bow	T_{bo}	m	0.1535	0.1385	0.111
Inner draft at bow	T_{bi}	m	0.1535	0.1385	0.111

Table 4.6 The calculation results of running attitude of SES 717C at various speeds

Item	Symbol	Units				
Craft speed	V	km/h	26.5	33.1	44.2	55.2
Cushion pressure	p_c	N/m^2	2813	2789	2776	2787
Flow rate	Q	m^3/s	5.115	5.115	5.165	5.15
Outer draft at stern	T_{so}	m	0.5254	0.5823	0.5952	0.5599
Inner draft at stern	T_{si}	m	0.2066	0.2008	0.1986	0.2006
Outer draft at bow	T_{bo}	m	0.086	0.0858	0.0868	0.089
Inner draft at bow	T_{bi}	m	0.086	0.0866	0.0868	0.089

Principal dimensions and parameters of the craft:

B_c = 3.5 m
B_{sw} = 0.13 m
B_{swb} = 0.06 m (width of the sidewall at bow)
H_{sw} = 0.42 m (height of the sidewall)
a_b = 70° (deadrise of sidewall at bow)
a = 60° (deadrise of the sidewall amidships)
S_a = 14 m^2 (frontal area of the superstructure)
a_s = 9.23° (inclination between the stern plate and base-line)
x_g = −0.47 m (aft amidships)
$\overline{KG}$ = 1.22 m
H_s = 0.50 m (height of thrust for water jet propulsion over base-line)

Dynamic transverse righting moment of the SES

Figure 4.23 shows the transverse righting moment M_θ of SES type 717C hovering statically and in motion. Figure 4.24 shows the components of dynamic righting moments M_θ of the SES type 717C running on cushion. It is found that the relative metacentric height h/B_c of the craft in motion is larger than that hovering statically by 20–30%. This added righting moment is mostly provided by the stern planing plate seal and it indicates that the craft type 717C is more stable when moving than when static. This has been validated in practice.

Further investigation

Transverse stability of craft during take-off

As mentioned above, the transverse stability of an SES at post-hump speed can be improved significantly with the hydrodynamic force on the stern seals of the planing plate type. It will deteriorate in the case of craft at low speed, particularly at hump

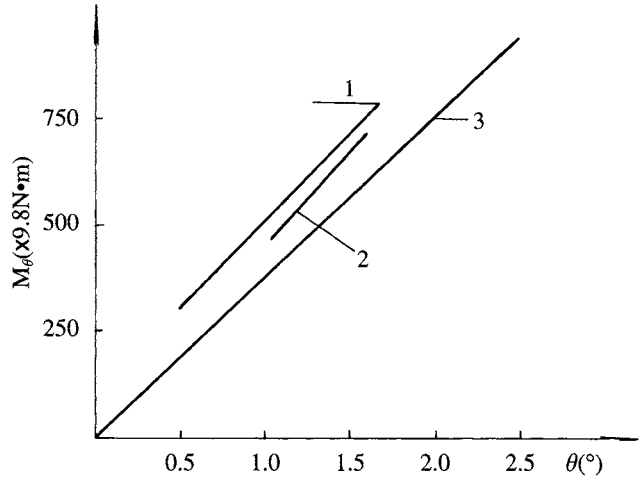

Fig. 4.23 Transverse righting moment of SES model 717C at different forward speeds. 1: v = 26.5 kph, h/bc = 0.439; 2: v = 33.1 kph, h/bc = 0.369; 3: v = 0, h/bc = 0.311.

speed. This was found both on model test and full-scale ship trials. This occurred to the SES type 717C with thinner sidewalls, which rolled violently at hump speed and even led to unstable yawing and plough-in. For this reason, it is very important to analyze the stability of craft during take-off.

Figure 4.25 shows experimental results of transverse stability of an SES model running at different speeds over water obtained by Soviet engineer A.Y. Bogdanov [44]. He presents the relative stability moment $M_\theta^v = M_\theta^v / M_\theta^0$, in which M_θ^v denotes the restoring moment of model at speed of v, M_θ^0 denotes the restoring moment of model at zero speed and Fr_D denotes the Froude number based on volumetric displacement of the craft.

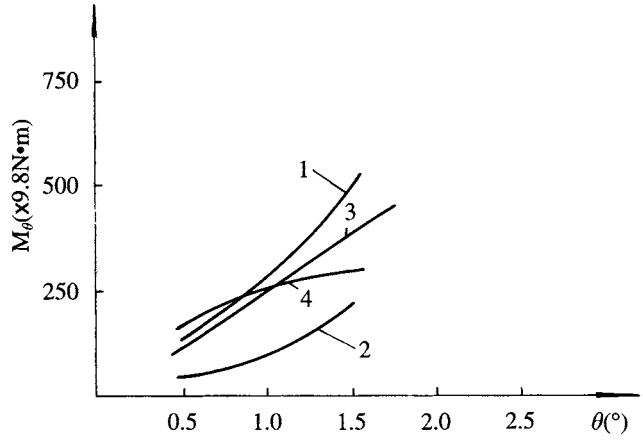

Fig. 4.24 Composition of transverse righting moment of SES model 717C. 1: Sidewall moment, $v = 44.2$ kph; 2: Stern planing seal moment, $v = 44.2$ kph; 3: Sidewall moment, $v = 26.5$ kph; 4: Stern planing seal moment, $v = 26.5$ kph.

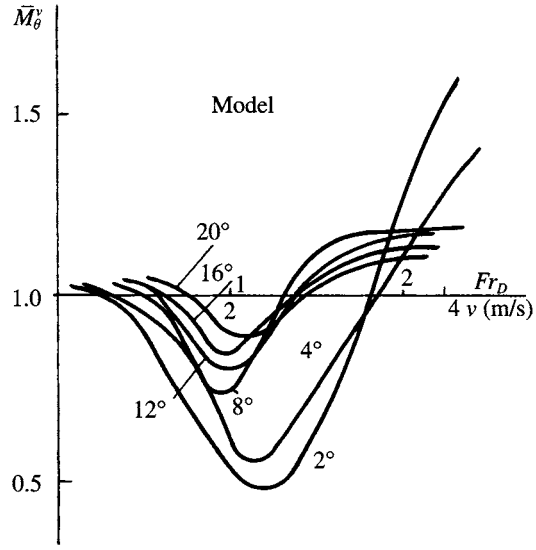

Fig. 4.25 Transverse stability moment of heeled SES at speed.

It can be seen that the transverse stability of the models reduces significantly during take-off, particularly in the case of small heeling angle $\theta = 2°$. The transverse stability even reduces to half of that at zero speed, though it increases rapidly above hump speed.

Bogdanov showed that the craft bow was situated at the wave peak and the stern at the trough when travelling at hump speed. The immersed sidewalls therefore cause added wave-making at this speed. When a craft is heeling this will cause a deeper trough at the stern for the immersed sidewall and in contrast, the trough would be reduced at the stern of the emerged sidewall. The restoring moment is therefore reduced due to such asymmetric drafts at both sidewalls and seals.

In the case where the craft speed is over the hump speed, the wave trough caused by the sidewalls and air cushion system will be far behind the craft stern and the immersed sidewall and seals will provide a large hydrodynamic force and righting moment. The transverse righting moment therefore increases rapidly at speeds above hump.

Transverse stability in waves

The transverse stability of hovercraft in waves needs to be considered together with craft motions, particularly with respect to the roll characteristics of SES in waves. This will be described further in Chapter 8.

Criteria and standards for the stability of SES

Criteria and standards for stability are a very important input to the design and construction of SES. The standards derived from various national bodies are described in Chapter 10. These vary somewhat. An approach to setting criteria is described below, based on Andrew Blyth's work for the UK CAA reported in [42].

Designs should always be evaluated at several loading conditions within the designed operating range, since this can often affect the results significantly. In order to address the differing needs of different stages of the design process, as well as the different levels of sophistication of analysis appropriate to craft ranging in size between tens and thousands of tonnes in displacement, compliance with each criterion may be demonstrated by a range of methods, ranging from simplistic formulae, through more complex mathematical methods, to model tests or full-scale trials (if appropriate).

Naturally, the more simplistic the method, the more important it is that the results can be expected to be conservative. So the use of more sophisticated and hence expensive techniques will often enable higher VCGs to be used with confidence. Failure to pass the simple methods does not necessarily imply total unacceptability.

Static stability

The initial, lateral roll stiffness averaged over the range 0–5° of heel should not be less than a transverse metacentric height (GMt) of 10% of the craft maximum beam, when measured or calculated for a static longitudinal trim angle within about half a degree of level keel. This is equivalent to a percentage CG shift per degree of 0.175. Calculation, model test or full-scale experiment are considered appropriate for evaluation.

Stability in waves

The SES should just be capable of surviving regular steepness limited waves (crest to trough height – 0.14 × wavelength) with breaking (as opposed to plunging) crests, of any individual height up to the limiting wave height, encountered beam-on while using full available lift power and combined with:

1. A TCG equal to twice the maximum normal TCG.
2. A beam wind as specified in the design environmental conditions. Special consideration of the safety margins would be required where this wind speed exceeds a velocity (knots, at 10 m high) equal to

$$15 \times B_c^{0.5} \text{ (in metres)}$$

The limiting wave height shall be taken as 1.9 times the significant wave height specified in the design environmental conditions.

An analysis of static on-cushion righting lever characteristics was conducted by Blyth to provide a relatively simple calculation method [42], although it was found that the minimum required properties of the curve vary substantially with hull configuration, due to the dominant effects of forcing and damping characteristics. Other acceptable methods of demonstrating compliance include mathematical simulations and model tests.

Stability in turns

Since the behaviour of an SES in high-speed turns is very dependent on both speed (which declines rapidly in tight turns) and the rate of turn achievable, the following criteria should be met when the vessel is at approximately 45° change of heading, in the test achievable turn, at a range of approach speeds within the operational range, for each weight condition to be considered. Note that behaviour is not always most critical at maximum speed.

1. The minimum net roll stiffness (expressed as minimum effective GMt) in the tightest attainable turn should always be greater than 5% of craft overall beam (Bc). This is equivalent to a percentage CG shift per degree of 0.087. This requirement need not be met if the total roll restoring moment in the upright condition is equivalent to an inward TCG greater than 2.5 times the maximum normal TCG, since this is considered to provide a good reserve beyond the maximum roll moments realizable in practice.
2. The net roll stiffness in a turn should not permit a greater outward heel angle than $(3 - Fn_c)^2$ degrees when the maximum normal TCG is applied in an outward direction where Fn_c = cushion Froude number = $V/(L_c \times g)^{0.5}$.
3. In order to avoid undesirable roll/pitch/yaw coupling effects, the hull form should be such that when a roll moment is applied at speed, any bow-down trim angle change should not exceed one-fifth of the heel angle.

Relatively simple calculation methods have been derived for assessment, but model tests are also acceptable and in many cases desirable. Some full-scale trials will always be required to demonstrate that the expected maximum rate of turn cannot be exceeded.

Commentary

It has been shown by Blyth's test programme that the on-cushion stability of an SES should be principally assessed in relation to rolling behaviour in synchronous beam seas and in relation to the hydrodynamic forces developed in high-speed turns.

In a seaway, capsizing of an SES is most probable in steepness-limited beam seas with a period close to resonance. An alteration in course and/or a reduction in lift power both substantially reduce the probability of capsize occurring. It has been shown that for each design, there is a VCG below which capsizing becomes improbable.

In high-speed turns, the hitherto unidentified possibility of large amplitude roll/yaw oscillations occurring has been detected and examined. It seems probable that this behaviour is associated with a zone of negative roll stiffness in turns, created by the manner in which hydrodynamic forces vary with roll attitude.

4.4 Calculation of ACV transverse stability

Introduction

An ACV has no natural restoring moment from the cushion (plenum chamber) itself while heeling on cushion. Air jet craft derived stability moments from the increased force of the jet on the downgoing side and reduced force on the upgoing side, though these were small and so such craft were very sensitive to movements of craft payload.

As an ACV heels, due perhaps to the movement to one side of a person on board creating an overturning moment, a negative restoring moment will act on the ACV if no other stability moments are created by deformation of the peripheral skirts, as shown in Fig. 4.26. This is because the cushion pressure will be the same across the craft width in the case of no cushion compartmentation.

The skirt geometry and in the case of skirts with pressurized loops or bags, p_l/p_c has a strong influence on the righting moment which is generated for an ACV. When travelling over water, the skirt stiffness will then affect the water displaced on the downgoing side, in a similar way to the action of SES sidewalls, below hump speed. Above hump speed, the skirt surface presented to the water acts as a planing surface, though the force that can be generated is limited to that which can be transmitted around the fabric membrane back to the craft's hard structure.

Cushion compartmentation

In the case where an ACV compartmented longitudinally hovers statically on a rigid surface, cushion pressure on the side heeling down increases due to reduced air flow and the cushion pressure decreases for the other side because of increased escape area and therefore flow rate. Thus the different cushion pressures give a direct restoring moment, moving the effective centre of pressure to the downward side of the craft, as shown in Fig. 4.27.

Meanwhile, the transverse component of $P_{c\theta}\sin\theta$ of the cushion pressure resultant $P_{c\theta}$ will also lead to a drifting motion. For this reason, drifting in general always

occurs with heeling. This phenomenon also happens on an ACV hovering on a water surface as shown in Fig. 4.28. In the case where the ACV heels on the water surface as shown in Fig. 4.28, the cushion pressures for left/right cushion compartments are rather different, thus it causes a different water surface deformation for each of the compartments. The water hollow under the left cushion compartment is deeper than that in the right compartment and the water displaced by the hollow is equal to the lift caused by the cushion pressure on each side. Thus it can be seen that the restoring moment and the drifting force are caused by the different cushion pressure in the left and right cushion compartments.

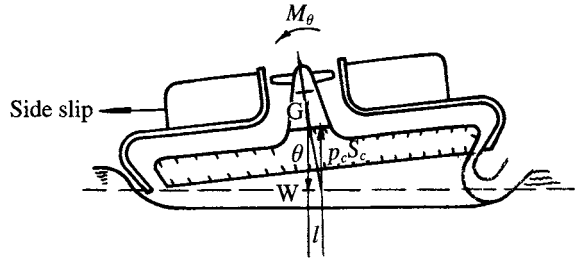

Fig. 4.26 Heeling of an ACV without air cushion compartmentation on water.

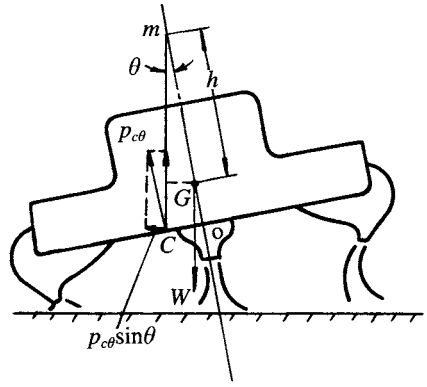

Fig. 4.27 Heeling of an ACV with air cushion compartmentation on rigid surface.

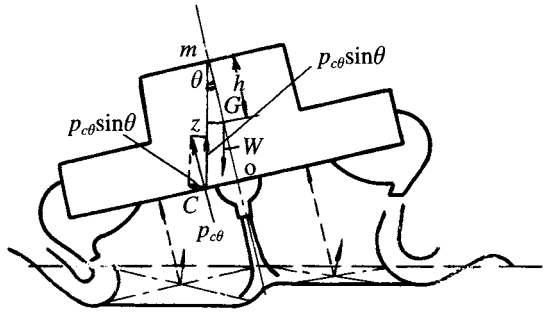

Fig. 4.28 Heeling of an ACV with air cushion compartmentation on water.

Separated bag or cell

Figure 4.29 shows the skirt configuration of the US ACV type JEFF(A). Since the air supply for left- and right-hand cells is separated, the pressure for the side heeling down will be increased in the case where the craft is heeling, and the pressure at the other side will be decreased, consequently causing a restoring moment. The French multi-cell skirt system (called the 'jupe' skirt) possesses the same effect as the JEFF(A) skirt system except that each jupe creates a moment independently.

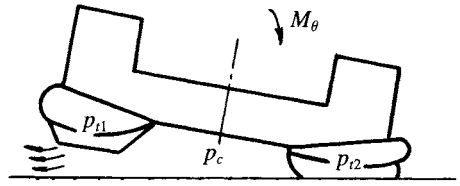

Fig. 4.29 Influence of pericell type skirt on craft stability.

Skirt lifting or shifting systems

The skirt shifting system and its principle of action was developed by Hovercraft Development Limited of the UK. The skirts might be shifted in the transverse direction to change the centre of pressure subsequently, to cause righting or heeling moments as shown in Fig. 4.30. Such systems have been mainly applied to move skirts side to side, particularly to allow a craft to bank into a turn. The system is convenient to install on a loop and segment skirt with the same pressure in the loop as the cushion, or with slight overpressure, 5–10%.

The British Hovercraft Corporation developed a simpler system for their bag and finger skirts whereby the segment is lifted, heeling a craft opposite to the external overturning moment. The geometry of a bag and finger skirt was found easier to deform by lifting and the effect was similar to that of the loop and segment skirt transverse shift system.

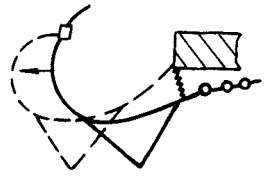

Fig. 4.30 Skirt with transverse shifting system for improving the transverse stability.

The transverse shift of centre of cushion area

The centre of cushion area may be shifted in order to produce a restoring moment, as shown in Fig. 4.31. When an ACV is heeling, the centre of cushion area will shift to the side which is heeling down (from C to C′ in Fig. 4.31) to offer a restoring moment.

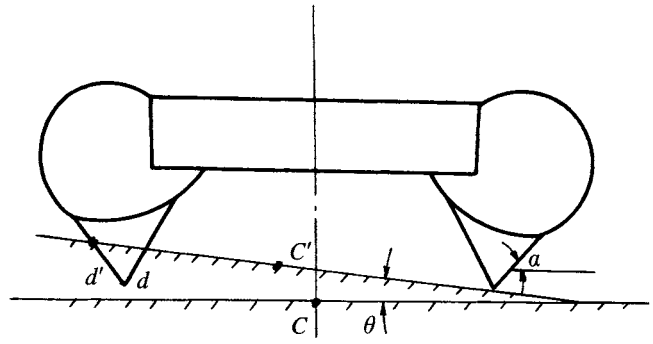

Fig. 4.31 Transverse movement of centre of cushion area of ACV with bag and finger type skirt on heeling. *c*, *c'*, centre of area; *d*, skirt contact with ground level; *d'*, skirt contact heeled.

Statically this may be estimated in two dimensions by determining the static equilibrium of the downgoing skirt as the ground point is raised from *d* to *d'*. In general this will result in just a small increase compared with the cruder assumption that the skirt does not move at all. The exception to this is if segments are replaced by pericells.

Larger ACVs (above around 5 t displacement) commonly use longitudinal and transverse stability skirts to improve craft stability; we will present analysis of stability including cushion compartmentation, with some additional guidance regarding the choice available to a designer to avoid such complexity.

Calculation of transverse stability for an ACV

It is very complicated to calculate the transverse stability of an ACV hovering over water because of the deformation of the water surface. The suggested analysis procedure is therefore to investigate the transverse stability of an ACV hovering on a rigid surface, followed by the corrections necessary due to the water surface deformation, obtained with the aid of model experiments.

The coordinate system and the basic assumptions can be written as follows:

1. Since the ACV is supported on a rigid surface, we neglect the effect of hydrodynamic force acting on the skirt and the deformation of skirts (i.e. we assume that the skirts are not deformable or at least have small deformations which can be neglected).
2. We simplify the cushion plane as rectangular and adopt a longitudinal stability skirt to compartmentalize the air cushion, assuming that the cushion pressure distributes uniformly both in left/right cushion compartments.
3. We consider the GXYZ system as the body coordinate system and the $0\xi\eta\zeta$ system as the fixed coordinate system as shown in Fig. 4.32.

The calculation method for predicting the static transverse stability of an ACV on cushion is very similar to that for an SES, i.e. in the case where the ACV is heeling, the lift due to the cushion pressure has to be equal to the weight of craft and the heeling moment equivalent to the restoring moment about the CG caused by the cushion pressure which satisfies the fan duct characteristic equation. The flow of the fan has

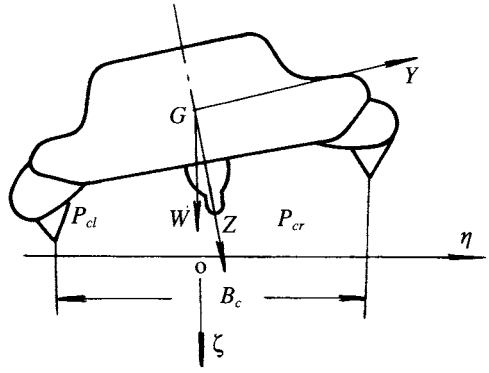

Fig. 4.32 Coordinate system of craft for stability.

to satisfy the flow rate continuity equation. Thus the equations of weight and moments can be expressed in matrix form as follows:

$$[A_n]\begin{bmatrix} P_{cl} \\ P_{cr} \end{bmatrix} = \begin{bmatrix} W \\ M \end{bmatrix} \tag{4.20}$$

where $[A_n]$ is the parametric matrix for cushion geometry of the craft and can be written as

$$[A_n] = \begin{bmatrix} A_{cl} & A_{cr} \\ A_{cl}Y_{pl} & A_{cr}Y_{pr} \end{bmatrix} \tag{4.21}$$

where W is the craft weight, M the heeling moment, $M = M_c + M_g$, M_c the righting moment due to the cushion pressure at the heeling angle of θ, M_g the heeling moment due to the height of CG at the heeling angle of θ, i.e. the moment of W about the intersection point of line GZ with the line linking to the lower tip of skirts, A_{cl} the area of left cushion, suffix l denotes left cushion, A_{cr} the area of right cushion, suffix r denotes right cushion, Y_{pl} the vertical distance between the CG and centre of left cushion area and Y_{pr} the vertical distance between the CG and centre of right cushion area.

The total pressure–flow rate characteristic of the fan and duct can also be expressed by

$$P_t = A + BQ + CQ^2 \tag{4.22}$$

where P_t is the bag pressure, Q the flow rate of the fan and A, B, C the parameters for fan characteristics.

Expression (4.22) defines the relation between bag pressure and flow rate. As a matter of fact, we have to put the total pressure of fan H_j into the foregoing equation instead of bag pressure P_t. Here we neglect the pressure of the air duct from the outlet of the fan to skirt bag. The bag pressure will be different in the case of different duct configurations. One has to consider this matter in practical calculations according to the specific geometry of the craft cushion air distribution system.

To simplify the calculation, we assume that one fan supplies the flow rate to both left and right cushions instantaneously and the pressure in both left and right cushions is equal. Thus the characteristics of cushion pressure and air leakage from bag holes can be expressed as

$$\begin{aligned} P_{cl} &= P_t - E_l Q_l^2 \\ P_{cr} &= P_t - E_r Q_r^2 \end{aligned} \tag{4.23}$$

where Q_l, Q_r, are the flow rates from left/right cushion, E_l, E_r the loss coefficient of bag holes in left/right cushion and P_{cl}, P_{cr} the pressure in left/right cushion.

From the flow rate continuity equation, we have

$$\begin{aligned} Q &= Q_l + Q_r \\ Q_l &= Q_{el} + Q_{lr} \\ Q_r &= Q_{er} - Q_{lr} \end{aligned} \tag{4.24}$$

where Q_{el}, Q_{er} are the flow rates leaking from left/right cushion and Q_{lr}, the cross-flow from left cushion to right cushion, can be written as

$$Q_{lr} = \phi\sqrt{(2/\rho_a)|p_{cl} - p_{cr}|}\,\mathrm{sgn}\,(p_{cl} - p_{cr})A_{eg} \tag{4.25}$$

where ϕ is the flow rate coefficient and A_{eg} the leakage area of cross-flow. A_{eg}, Q_{el} and Q_{er} in the above equations are related to the air leakage gap; they are a function of heeling angle θ.

In the case where one side contacts the ground, the cushion area of this side kneeling down may be determined as follows. Figure 4.31 shows the contacting point of the skirt with the ground, d, in the case of a craft where the skirt touches but is not deformed. This will be shifted to d′ in the case of heeling craft due to the skirt kneeling down, the cushion area at this side (skirt kneeling down) will increase in order to provide the restoring moment.

The contacting point is related to the outer surface inclination angle of the skirts, a. The righting moment is inversely proportional to a. These effects have been considered in equation (4.21). The equation group in this section is called the coupled stability equation for heeling and heaving of ACVs, which is very similar to that for SESs.

In the case where the heeling moment (force), principal dimensions of the craft and the leading particulars for fans, skirts and cushion are given, then the parameters such as P_{cr}, P_t, Q, Q_{ei}, Q_{er}, Q_{lr} can be solved with aid of a computer and the expressions (4.20)–(4.25). The heeling angle θ as well as the vertical position of CG (ξ_g) can also be obtained.

Figure 4.33 shows a typical curve of static transverse stability of an ACV hovering on a rigid surface. It can be seen that the curve is nonlinear at larger heel angles, due to the nonlinear factors of fan characteristics and ground contact and deformation of skirts.

4.5 Factors affecting ACV transverse stability

Based on the equations mentioned above, one can discuss the effect of the various parameters on the static transverse stability of an ACV. However, the errors of calculation are rather large since no account is taken of the deformation of skirts caused by the

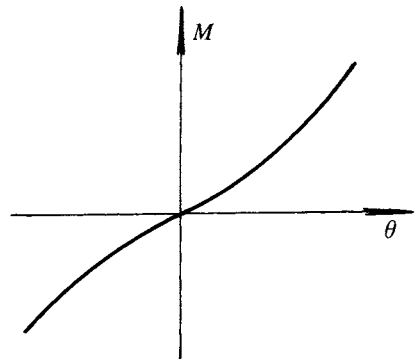

Fig. 4.33 Typical static transverse stability curve for ACV.

change of cushion pressure of the craft in heeling and the effectiveness of the air cushion blown from the nozzle of stability skirts on the stability of craft.

Therefore these problems have to be solved by experiments. References 45 and 46 offered some commentary on experimental results from model tests as discussed below.

Effect of supporting surface

Figure 4.34 shows that the static transverse stability for an ACV model with + type of cushion compartment hovering on a water surface is worse than that on rigid surface due to the deformation of the water surface. In general the static transverse stability on the water surface is about 70–80% of that on rigid surface whatever type of cushion compartment was adopted.

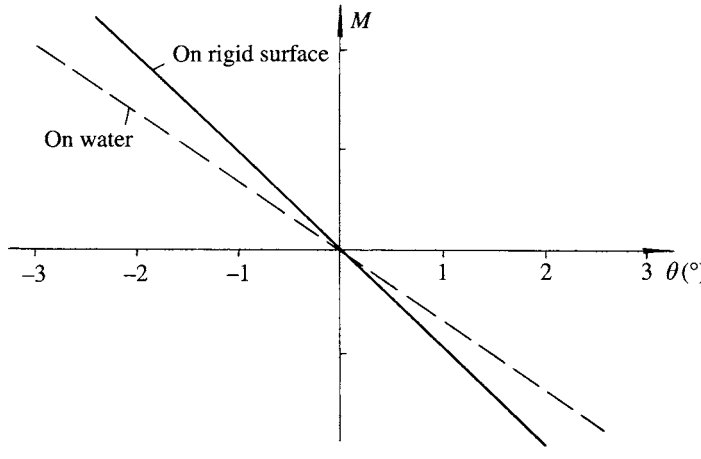

Fig. 4.34 Static transverse stability of ACV models with + type of air cushion compartmentation.

Transverse stability of an ACV without the cushion compartmentation

An ACV without the cushion compartmentation can also provide a positive restoring moment during heeling of the craft. This is due to the skirt finger with so small an inclination angle as to change the centre of cushion area and provide a positive restoring moment, as the skirt contacts the supporting surface during heeling of craft. Figure 4.35 shows a typical static transverse stability curve of an ACV without compartmentation.

With respect to ordinary ACVs, the restoring moment is due to the following factors:

1. The restoring moment is due to the cushion compartmentation inducing different pressure in different cushions. This is called compartment stability.
2. The restoring moment is due to the change of cushion area, either arising from the inclination angle of skirt fingers, or from the deformation of the skirt in the horizontal direction. This is called area stability or stability due to ground contact of the type of cushion compartment on static transverse stability of an ACV.

Figure 4.36 shows the effect of three types of cushion compartment on static transverse stability, in which l_g denotes the length of longitudinal stability skirt (measured from stern); therefore, $l_g/l_c = 0$ denotes that without cushion compartment; $l_g/l_c = 0.6$ denotes compartmentation of T type, and $l_g/l_c = 1.0$ denotes + type compartmentation.

The criterion for transverse stability can be written as

$$\bar{S}_R = [\Delta M/\Delta\theta] / [WB_c] \tag{4.26}$$

where $\bar{S}_R$ is the relative shifting distance of centre of pressure per unit heeling angle. This criterion is equivalent to the relative height of initial stability:

$$\bar{h} = h/B_c = [\Delta M/\Delta\theta \times 57.29] / [WB_c] = \bar{S}_R \times 57.29 \tag{4.27}$$

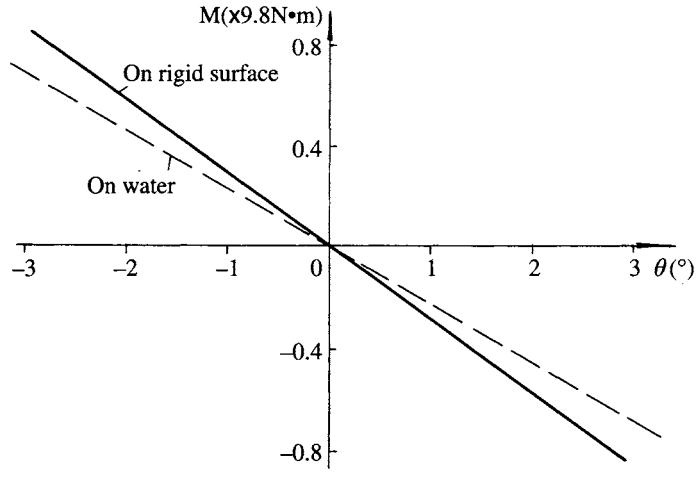

Fig. 4.35 Static transverse stability of ACV models with no air cushion compartmentation.

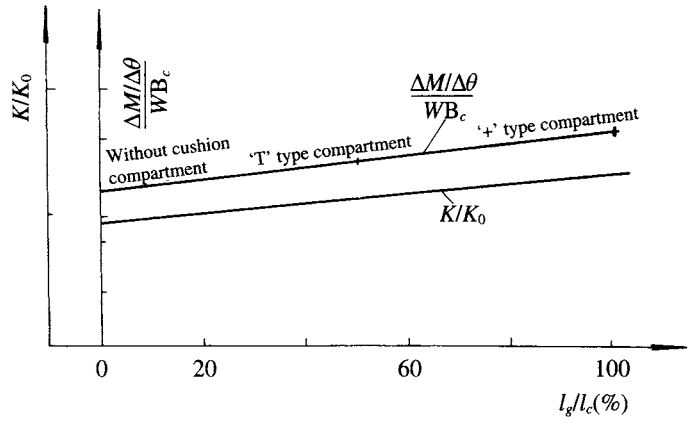

Fig. 4.36 Influence of air cushion compartmentation on static stability.

where $\Delta\theta$ is the heeling angle (for a small value) (°), ΔM the restoring moment (N m), h the initial transverse metacentric height (m), W the craft weight (N) and B_c the cushion beam (m).

K/K_0 (in Fig. 4.36) shows the effect of the depth of the stability skirt on transverse stability. It can be seen that the stability of an ACV without cushion compartmentation will be reduced to about 60% of that with the + type of cushion compartment. Reference 47 demonstrated experimental results such that the transverse stability would be decreased to 59% in the case of removing the longitudinal stability skirt and the longitudinal stability would be decreased to 68% in the case of removing the transverse stability skirt.

It is clear that this investigation is very important and plays a key role in analysing the stability of an ACV. Since transverse and longitudinal stability skirts are normally situated inside the cushion and are very difficult to repair and maintain, it is more convenient to remove stability skirts if at all possible. While this is now practical, it has take some years for skirt design technology to advance to the point where satisfactory stability can be provided (see Chapter 7).

Figure 4.36 also shows that the transverse stability for the craft with T type compartment will be decreased to 85% of that with + type compartment.

Effect of stability skirt clearance h_{ej} on the transverse stability

Stability skirt clearance has a direct effect on the effectiveness of cushion compartment and transverse stability. Figure 4.37 shows that the role of the cushion compartment will decrease as the stability skirt clearance h_{eg} increases to larger than 30% of cushion depth at CG. In general, h_{eg} is equal to 10–20% cushion depth at CG, but stability skirts of + type are more sensitive than those of T type.

Effect of VCG on transverse stability

VCG has a clear effect on transverse stability of craft. Figure 4.38 shows that VCG is directly related to height of skirts, therefore one has to make a comprehensive

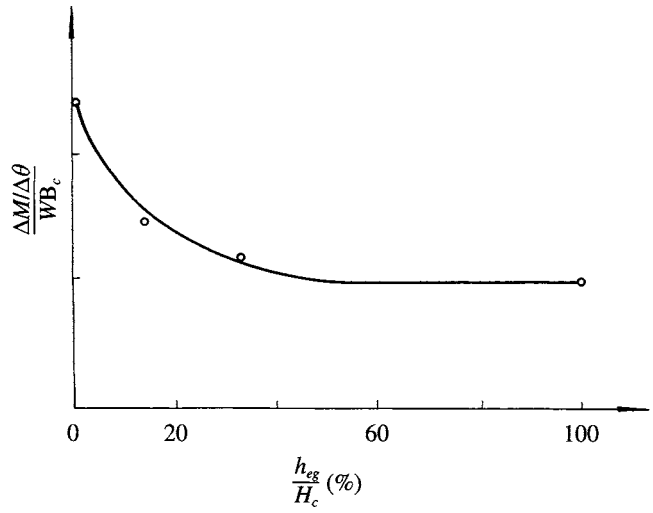

Fig. 4.37 Influence of gap between the lower tip of transverse stability skirt and ground on static transverse stability of model craft.

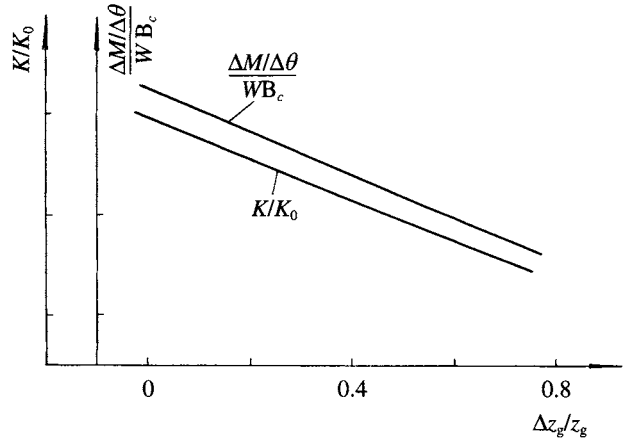

Fig. 4.38 Influence of vertical position of centre of gravity on static transverse stability.

analysis of transverse stability during the design of skirt height. If one uses higher skirts due to the requirements of obstacle-clearing capability and seaworthiness, then effective measures for stability have to be adopted during the design stage.

Effect of fan flow rate on transverse stability

Figure 4.39 shows that transverse stability of an ACV is directly proportional to the flow rate of fans, the relation of which is opposite to that for SES. Probably the rationale of this phenomenon is that the slope of total head with respect to the flow rate on a characteristic curve increases as the flow rate of the fan increases, which leads to enhanced transverse stability.

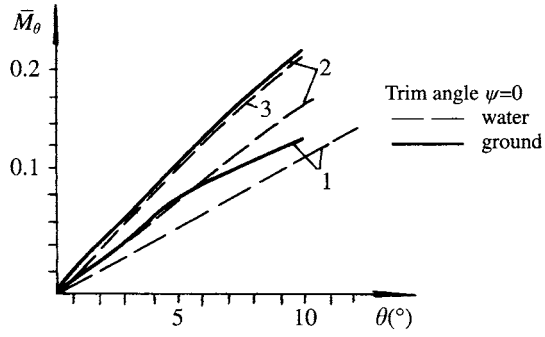

Fig. 4.39 Influence of air flow rate on static transverse stability. 1: lift for speed n = 3000 rpm; 2: n = 4500 rpm; 3: n = 5000 rpm.

4.6 Dynamic stability, plough-in and overturning of hovercraft

Introduction

We will now introduce the dynamic stability of ACVs travelling over water. During the early development of ACVs (see Chapter 1) hovercraft had very limited stability. The concept being developed was to use air jets to allow these machines to 'fly' close to the ground. This approach had to be revised once flexible skirts were introduced.

When operating over water, particularly at speed, the forces induced from wetting of the lower part of the skirts could produce significant changes of trim. The early design of skirts was such that these changes of trim did not create additional righting moments, but instead they were reduced. Unless the hovercraft pilot took action to maintain level trim, the craft would eventually plough-in and either come to a stop, or overturn.

There were a number of overturning accidents in those early days. As an example the Chinese experimental ACV type 711 overturned during a trial in May 1966. The craft was travelling at the speed of 50 km/h and had to make a sudden turn in order to avoid collision with a small boat. When the craft made the turn, yawing and heeling to a large angle occurred, and the craft capsized.

Some British ACVs also overturned at a high speed on calm water. The process of capsizing was as follows: bow pitching down, drifting, yawing and combined heeling, high-speed plough-in and then overturning. Figure 4.40 shows plough-in of the British ACV SR.N6 and Fig. 4.41 shows the plough-in that induced the capsizing of a radio-controlled ACV model recorded by cine camera.

The sequence of plough-in events was stated in the driver instructions of SR.N5 as follows:

> Contact of the flexible skirts with water surface leads to a bow pitching down moment and bow pitch down, which will be magnified as the water resistance increases at increased speed. The features of the plough-in phenomenon are

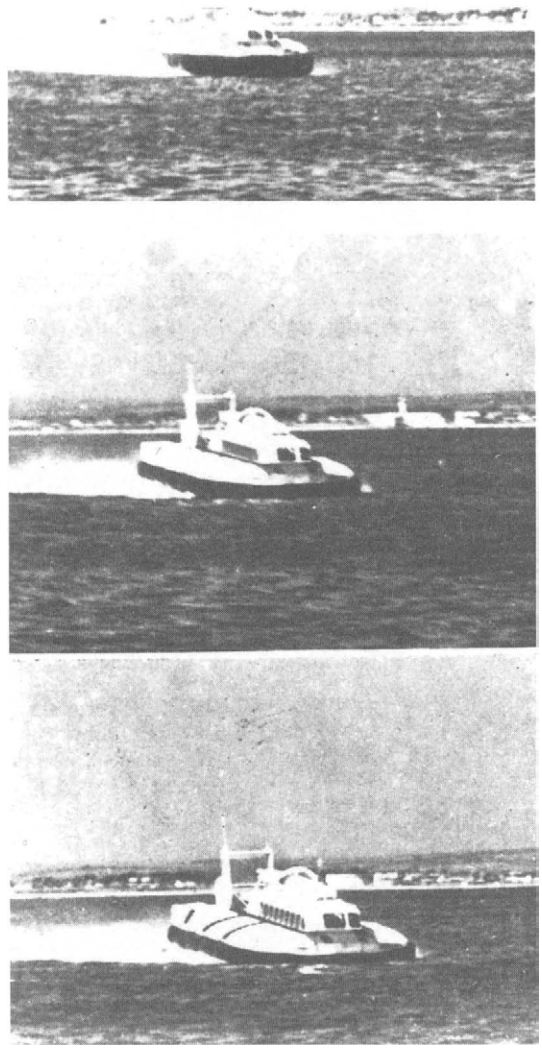

Fig. 4.40 The plough-in phenomenon of British SR.N6 in tests.

that the speed decreases, followed by large pitching down and heeling angle, as well as stern pitching up tendency so as to enlarge the drifting angle.

The principal author has had a number of such experiences; for example, the 5 t ACV model 711–II would plough-in on calm water (or in a breeze) at a speed of 70–80 km/h. In the case where the craft was travelling downwind, then the probability of plough-in would be over 90%. Violent slamming would occur to the craft and lead to speed degradation from high speed (about 80 km/h) to off cushion speed (about 5 km/h) in 2–3 seconds. Such high deceleration accompanied by the

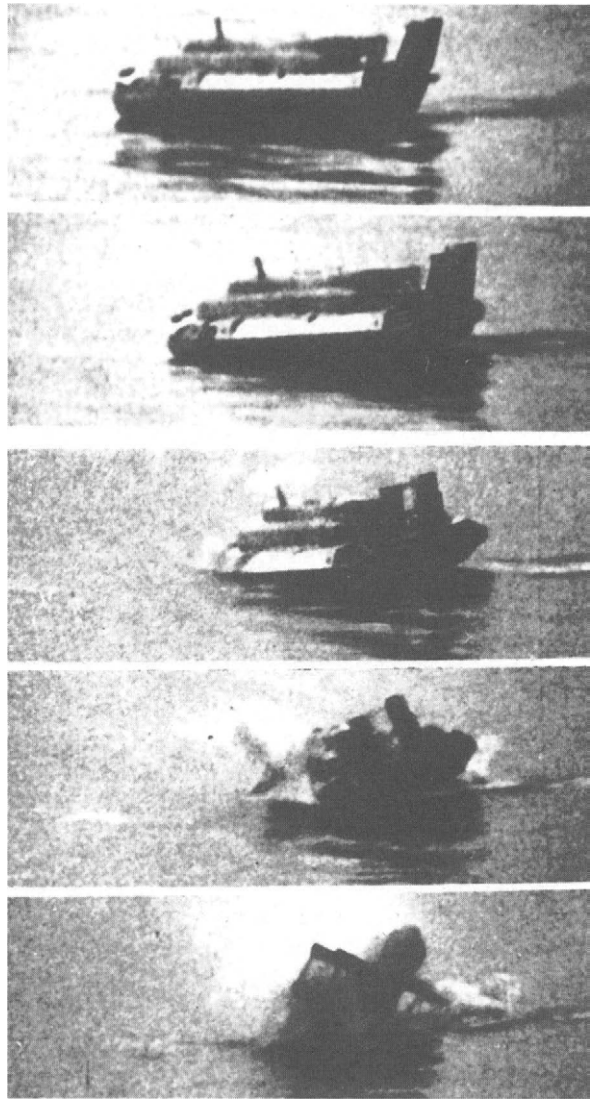

Fig. 4.41 The overturning of a hovercraft model recorded by cine camera.

slamming would lead to the skirt being damaged, engine mountings destroyed and people injured. This same phenomenon has occurred on a number of other Western and Chinese domestic ACVs in the mid 1960s to 1970s.

Similar phenomena have also occurred to SES at very high speeds, for example the US Navy SES–100A at a speed of over 70 knots. But in general it is seldom experienced. The plough-in of an SES downwave will be described in Chapter 8.

On smaller craft, with which the second author has considerable experience, the trimming moments generated by payload movement (i.e. passenger movement) can

significantly affect trim. As a result it is possible to experiment with a craft in suitable conditions, to test the stability of a bow or side skirt at different speeds. Beyond a small bow-down trim (1–2°) most skirts begin to wet (i.e. air flow is partly blocked and some of the segment surface is not lubricated by the air flow), leading to a sharp rise in drag. The beginning of this process can be seen on skirts without a swept-back bow, as the segments or bag appear to 'nibble' which can be seen directly or via movement of the loop. Beyond a further small trim-down, the rate of increase of drag causes rapid deceleration of the craft and in the case where the skirt system is not stable, either plough-in or overturning.

Sideways drift can cause a similar effect on the side skirts. Payload (CG) shift away from the drift to bank the craft can be very helpful. In this respect, provision of elevators or skirt shift mechanisms on utility size craft can be very important in maintaining dynamic stability. The CG shifts required are too great and required too quickly for larger craft, which have to rely on cushion compartmentation to keep the skirt stability envelope outside the normal operating conditions.

The increasing hydrodynamic force (and moment) due to contact of the flexible skirt with the water surface is the main reason leading to plough-in.

Before development of special skirt geometries, plough-in could be avoided only with aid of driver operating rules formulated by users, or research and design bureaux. Thus it can be seen that it is very important to study the rationale of plough-in and the overturning phenomenon.

Some ACV plough-in and overturning incidents will be examined below and a rationale developed. We will not present a theoretical analysis of this field due to its complicated hydromechanics. Readers may find [48] useful as background material, developed by the UK Department of Transport after the SR.N6 accident in 1973.

ACV overturning at low speed

In a similar way to an SES, the trough is so deformed on the water surface underneath an ACV during take-off as to reduce the stability skirt effectiveness. Figure 4.42 shows the inner water surface of a two dimensional ACV model at various Fr; it can be seen that the trough is deep at $Fr = 0.5$–0.7, which causes the detrimental influence on the transverse (or longitudinal) stability of the craft.

Figure 4.43 shows results of an investigation by W.A. Crago. He found that the transverse stability deteriorated dramatically at $Fr_1 = 0.33$–0.56. Figure 4.44 shows that the heeling moment and heeling angle increased at $Fr_1 = 0.4$ and the craft would capsize at overturning moments exceeding $M_\theta/(WB_c) = 0.022$.

For this reason, as far as the drivers are concerned, great attention is required during take-off, particularly in the case of long time duration for take-off due to shortage of lift and propulsion power, or if for other reasons the craft stability is low, due for example to a large amount of free surface liquid existing on the craft.

As far as designers are concerned, attention has to be paid to design skirts with a stable geometry for the hydrodynamic forces expected at hump speed and a realistic range of overturning moments and resultant craft trim.

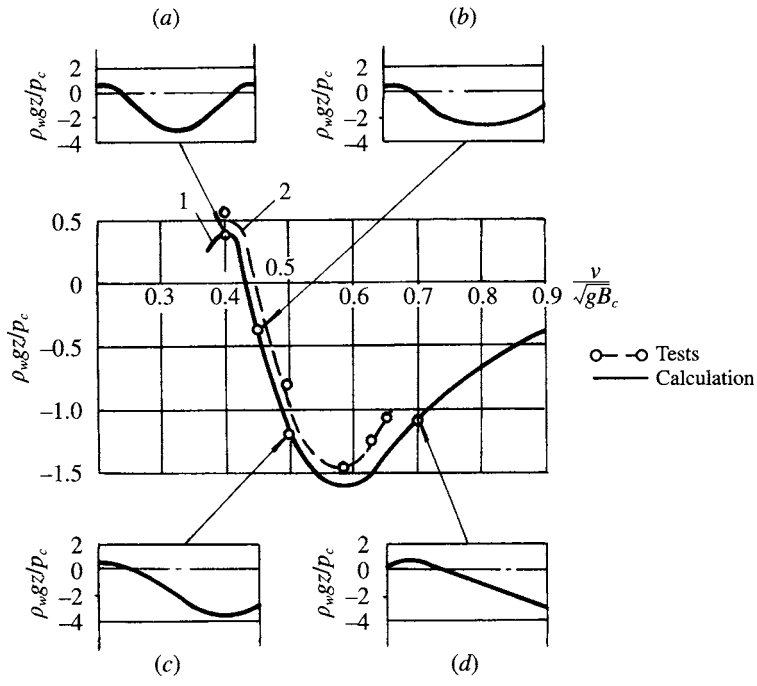

Fig. 4.42 Internal wave profiles of two dimensional ACV at different Froude Numbers. (a) $Fr_B = 0.4$, (b) $Fr_B = 0.44$, $Fr_B = 0.5$, (d) $Fr_B = 0.7$.

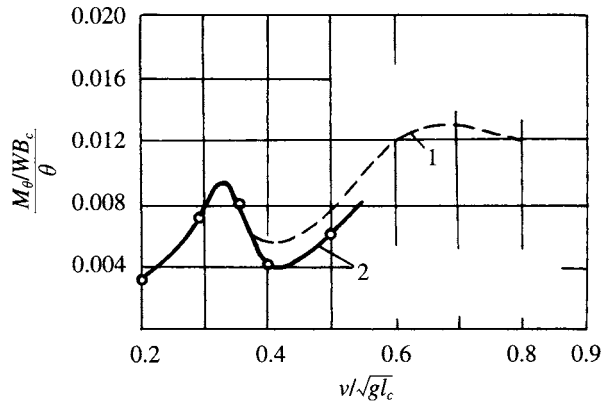

Fig. 4.43 Variation of transverse stability of ACV model as a function of Froude Number. 1: calculated from craft trim, 2: calculated from 2D cushion pressure distribution.

Plough-in and overturning of craft running at high speed

ACVs can normally be led into instability while travelling at high speed as shown in Figs 4.40 and 4.41. It is primarily due to bow down trim, or for some craft level trim, due to the aerodynamics of their body shape.

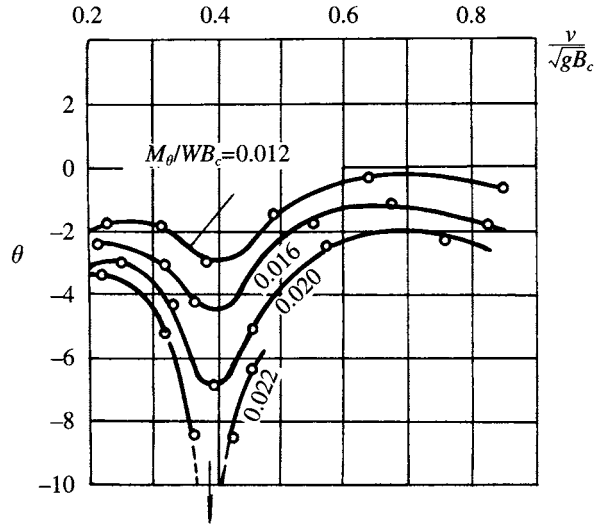

Fig. 4.44 Experimental results of rolling angle of hovercraft models as a function of craft speed.

Bow pitching down and plough-in are common terms used by the hovercraft designer often without clear distinction between them. The former means the craft bow pitching down at the bow skirt but still in a condition where the skirt segments are air lubricated and 'plough-in' means the craft is pitching bow down with so large a negative angle as to lead the skirt undergoing significant wetting giving large local drag forces and accompanied by the tuck-under of the bow skirt. Here we will investigate this problem in three phases, i.e. the progression, the reasons and the measures for improvement.

The progression during plough-in

The typical progression at plough-in can be described as follows (Fig. 4.45):

- Fig. 4.45(a): An ACV normally travels with a definite positive trim angle (bow up), and spray blown out under the fingers of bow skirt can be observed.
- Fig. 4.45(b): As the craft speeds up, the positive trim angle decreases as the thrust of the air propulsor increases. In the case where the craft is travelling downwind and a gust occurs, this causes the thrust to increase suddenly and lead to contact of the bow skirt fingers with the water surface. Meanwhile the spray blown from the delta zone between the tips of the skirt fingers can also be observed. The craft is still running with positive stability.
- Fig. 4.45(c): Hydrodynamic resistance increases as the wetted surface of skirts increases, thus the dynamic pressure of oncoming flow on stagnation will be so balanced by the cushion pressure, as to lead to the deformation of skirt fingers and cause the skirt to plane without spray. Eventually this can produce a suction acting on the skirt fingers, which leads to the fingers actually touching the water surface.

  The hydrodynamic drag increases further, light tuck-under occurs on the fingers, leading to the bow cushion being pulled back and the cushion area decreased. Subsequently the total force from the cushion drops while the cushion pressure rises

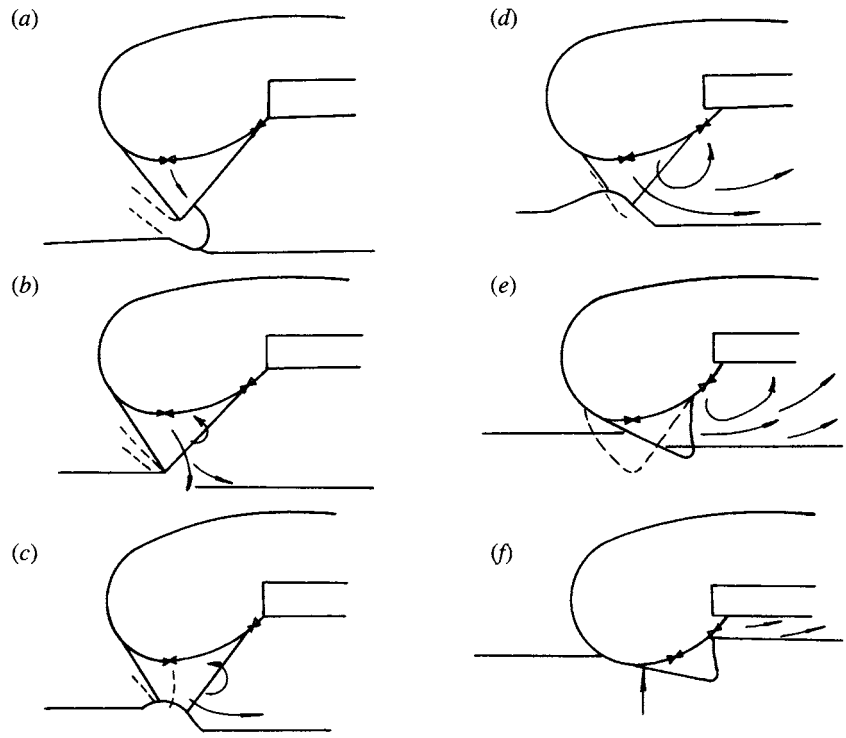

Fig. 4.45 A typical overturning process for an ACV.

and the skirts are immersed further in the water, building up drag on the bow skirt. Longitudinal stability deteriorates.

- Fig. 4.45(d): Following the situation in Fig. 4.45(c), the bow skirt tuck-under increases and craft trims further bow down. While there is still dynamic equilibrium at this point, the longitudinal stability deterioration is self perpetuating and this is the sign for plough-in.

  The plough-in phenomenon can be avoided if the driver takes measures at this point to reduce bow down trimming moments; for instance, throttle down on propulsion engines to bring the bow up; open to full throttle on lift engines; operate the horizontal rudder or air duct valve to raise the bow trim.
- Fig. 4.45(e): The wetted area of the bow fingers increases so as to increase the skirt drag violently, meanwhile the underfeed at the bow increases so seriously and strength of the flow vortex increases due to a large speed of cross-flow out to the side of the skirts, and decrease of cushion pressure at the bow and a large moment for pitching bow down, consequently the slamming of craft due to the plough-in occurs in a short period of time.
- Fig. 4.45(f): During plough-in and slamming of the craft, the bow skirt contacts the water surface producing a large hydrodynamic lift. Although a large negative acceleration occurs to the craft, the craft is still moving forward due to the inertia force, which strengthens the suction of the bow skirt and increases the bow cushion negative pressure to maximum absolute value. In the case where the plough-in and

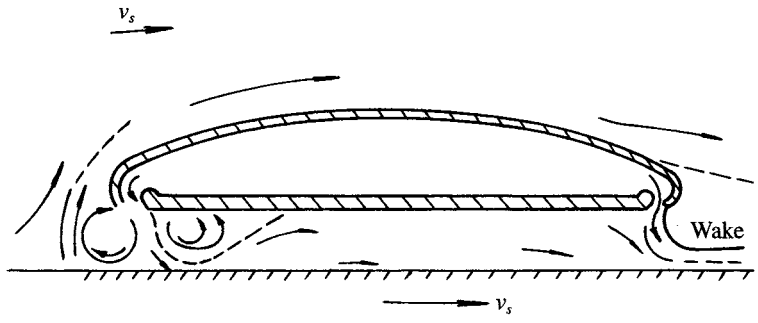

Fig. 4.46 Internal and external air stream lines of a high speed hovercraft model.

slamming occur together with drifting and slipping, then the craft may capsize, if the driver does not take any measures to prevent it.

Principal reasons for plough-in and overturning

Table 4.7 shows the main test data recorded during plough-in of a test craft.

1. The air stream ram pressure increases as craft speed increases, which leads to the sealing action of the cushion outflow (Fig. 4.46) [49]. Thus jet underfeed and cross-flow occur in the cushion, which will be accelerated due to the effect of the boundary layer under the cushion. Thus it can be seen in Fig. 4.47 that the bow cushion pressure decreases and stern cushion pressure increases as the craft speeds up, which lead to the centre of pressure being shifted to the stern. This is probably the internal reason for the plough-in.
2. Since the air propulsors of an ACV are mounted on the upper deck or superstructure, the thrust line is generally high over the supporting surface, therefore the thrust overturning moment increases as the speed increases, and will be magnified in the case of travel downwind. Thus a bowpitching down moment acts on the craft, which we consider to be the external reason for the plough-in. Figure 4.48 shows the experimental results of models running without drifting motion carried out by Crago [50], in which T/W_n denoted thrust/lift ratio. Clearly the region of plough-in increases as thrust/lift ratio increases.
3. Owing to the internal and external reasons mentioned above, the bow skirt contacts the water surface, leading to tuck-under of the skirt as the craft speeds up and during

Table 4.7 The main test data in the course of plough-in of a test ACV

Time (s)	Trim angle	Bow cushion pressure	Stern cushion pressure	Situation
1 – start	1.78	1160	1130	Normal travel
2	1.08	1200	1100	Finger contacts water surface
2.5	0.90	1180	1100	Light tuck-under
3	0.62	1150	1100	Moderate tuck-under
3.5	0.03	1050	1040	Serious tuck-under
4	−0.05	900	950	Tuck-under unstable
4.5	−1.16	250	630	Plough-in begins
5	−3.94	−1200	350	Bow structure touches
5.5	−1.14	−1000	600	Recovery of skirt
9 – end	+1.60	1200	1130	Normal trim

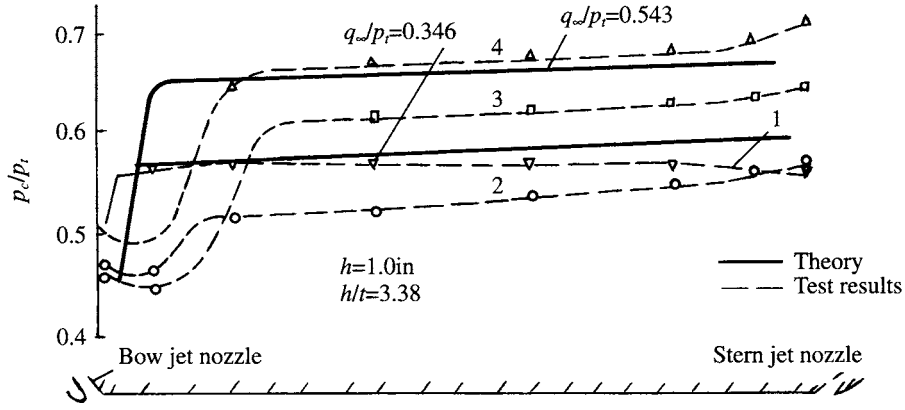

Fig. 4.47 Cushion pressure distribution vs ship speed. 1: $q_\infty/p_t = 0$, 2: $q_\infty/p_t = 0.346$, 3: $q_\infty/p_t = 0.543$, 4: $q_\infty/p_t = 0.743$.

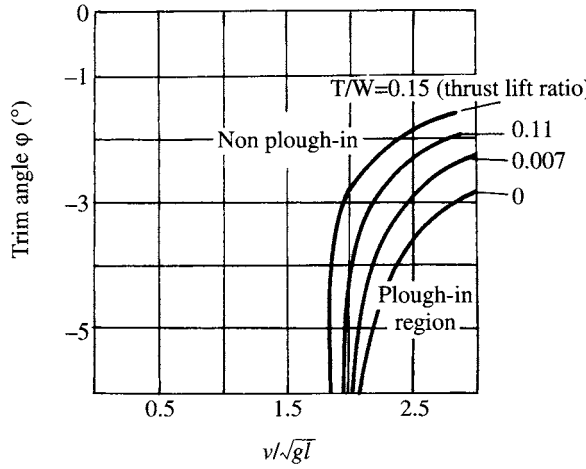

Fig. 4.48 Relation between the ACV plough-in boundary and trim angle, Froude numbers, thrust/lift ratio.

travel downwind, the area of the bow cushion decreases; meanwhile, the hydrodynamic drag on the bow and side skirts increases rapidly, which leads to increased bow pitching down moments, consequently the vicious circle concerned with drag and pitching bow down moments occurs, finally leading to capsizing of the craft.

Figure 4.49 shows the hydrodynamic lift moment increasing with the angle of the bow pitching down, which gives a restoring moment and the increased bow skirt drag (which causes the bow pitching down moment), as well as the cushion pressure reduction.

To sum up, the total bow pitching down moment increases with the angle of the bow pitching down, which may be seen in Fig. 4.49. Therefore the tuck-under of the bow skirt caused by the bow pitching down moment will normally be the direct reason causing the plough-in.

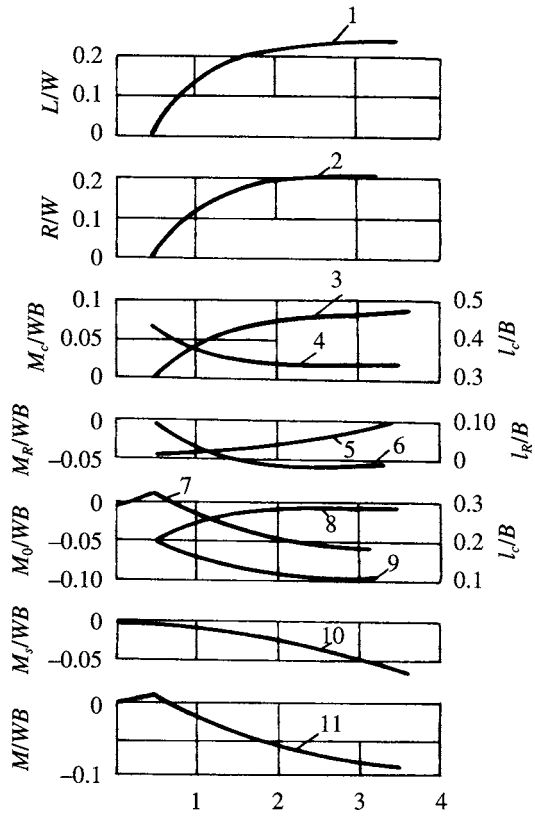

Fig. 4.49 Relation between various recorded forces on craft and trim angles. 1: Bow skirt, 2–6: bow skirt, 7: moment ratio due to *pc*, 8: moment ratio, rear cushion, 9: moment ratio fore cushion, 10: moment ratio, spray drag, 11: overall moment ratio.

4. In the case where the plough-in occurs with drifting motion, the resultant of such action might lead to capsizing of the craft. A large heeling angle and subsequent capsizing of the craft will be even more likely as a result of a high-speed plough-in while the craft is also drifting. Table 4.8 shows the speed range which might cause plough-in and capsizing [50]. It may be seen that the plough-in might occur in the case of $Fr < 0.7$, and it might lead to overturning if the drift angle was larger than 50°.

   This represents the experimental results from work carried out by Crago at the end of the 1960s. Owing to designers' efforts in recent years, the speed range where

Table 4.8 The speed range of ACV and *Fn* in which the plough-in and capsizing of craft may occur [48]

Items	High speed	Moderate speed	Low speed
Froude number Fn_B	1.7 or more	0.5–1.7	0.4 or less
Plough-in start	Probable	Impossible*	Impossible
Overturning	Probable in the case of drifting angle larger than 50°	Low probability	Probable according to motion records

* It is very difficult to overturn the ACV, but plough-in might be initiated in this speed range in the case of plough-in of craft at high speed and dropping down to this speed range.

positive stability is practical has been greatly extended, and sensitivity to plough-in and capsizing has been significantly reduced.

Figure 4.50 shows the relation between craft capsizing and drifting angle, in which the solid line denotes the position of the craft during turning using air rudders at the beginning of turning and then keeping the rudder in a central position. It can be seen that the drift angle remains stable. The dashed line denotes the position of the craft during turning using the rudder at a constant angle from the beginning to the end of turning. Here it can be seen that the ACV overturned at the drifting angle of approximately 70°.

Measures for improving resistance to plough-in and overturning

(A) Cushion and skirt air supply system

1. Keep a definite reserve on fan inflow rate and so increase the speed of fan, air gap, especially, the air supply flow rate at bow. If necessary, to increase the bow air gap and restore the running attitude to normal (in time), in the case where the craft develops a bow pitching down trim. It is very effective to provide a special air duct to supply pressured air to the cushion at the bow in order to improve the plough-in resistance. This has been validated by model experiments and modifications to many ACVs in the UK as well as China.
2. Use a separated duct system (or separate fan(s)) for supplying the pressured air to fore and rear cushion and skirt bags or loops.
3. Improve the cushion compartmentation for fore and rear cushion.

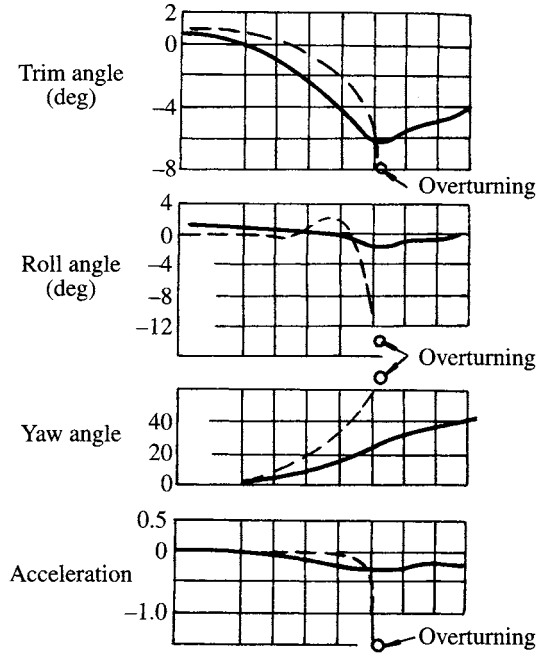

Fig. 4.50 Influence of yawing angles on the overturning of craft.

4. Increase the bag–cushion pressure ratio of skirt bags and the bow skirt separately if the bag is divided, to increase the stiffness of the bag of the bow skirt.

(B) Skirt systems

1. Install diaphragms in a D-type skirt bag at the bow to enhance the ability to prevent tuck-under. Figure 4.51 demonstrates the experimental results of a skirt carried out on a water circulating tank, which predicts in quality the effect of the tightness of a D-type bag and its diaphragms on the plough-in resistance of the craft. This is one of the general measures for plough-in resistance which is currently widely adopted in China.
2. Decrease the drag due to the contact of the skirt fingers with the water surface to prevent tuck-under of the bow skirt fingers.

   A large number of small air lubrication holes were fitted at the lower hem of the bow bag of the British SR.N6, so that air leaking from the cushion through the holes and along the outside of fingers at the water surface lubricated the contacting surface of the finger with the water surface and reduced the drag dramatically at a negative pitching angle, reducing the tuck-under of the fingers as shown in Fig. 4.52.

   This idea has not been developed further, as BHC redesigned the bow bag of later skirts, moving the fingers forward and increasing the bow bag radius (the bulbous bow bag). This skirt geometry creates increasing stability moments as the bow is trimmed down and so has 'safe' plough-in characteristics – see Chapter 7.
3. Careful manufacture of the skirt, to give an even bag or loop hem line and even segment or finger tip line (tidy the skirt geometry) decreases the dynamic drag, especially at the rear corners and reduces uneven loads within the skirt, which can contribute to ACV instability.
4. Adopt skirt-lifting equipment to control the height of the stern skirt, and so the trim angle of the craft.

(C) LCG Include ballast tanks, horizontal fins and duct valves, etc. to control the trim angle of the craft, especially in the case of travelling downwind, to increase the ability to trim bow up dynamically.

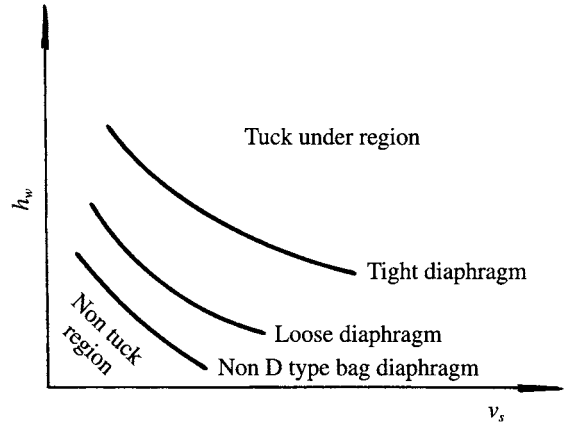

Fig. 4.51 Influence of craft speed, immersion height of skirt fingers h_w and the tightness of diaphragm of D-type skirt bags on plough-in of craft.

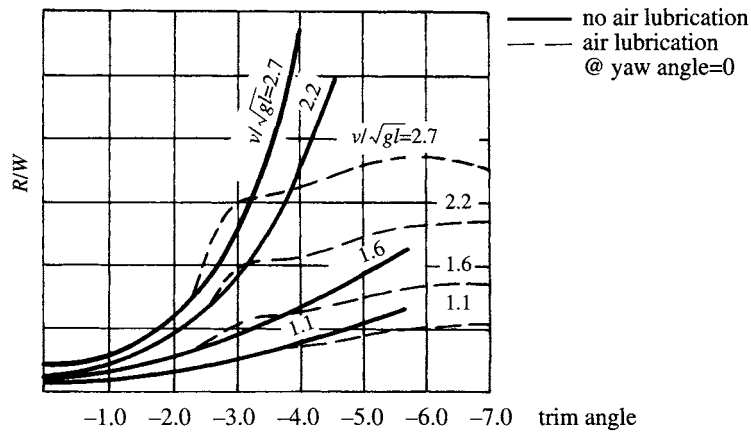

Fig. 4.52 Relation between the lift-drag ratio and trim angle of ACV.

(D) Driver technique Improve the drivers' technique for preventing the plough-in of craft and understanding the operational boundary curve for avoiding plough-in. Figure 4.53 shows the operational boundary for preventing plough-in on British ACV model SR.N6. Drivers have to take care during operation to avoid large drifting angles for overturning.

(E) Hull design It is not possible to completely avoid the possibility of plough-in on an ACV or SES. The designer should therefore investigate the attitute of the lower hull in the case of a bow-on or side-on collapse of the leading skirt. The hull lower plating, or the configuration of the deflated skirt drawn back over the hull structure, should form a planing surface with between 5 and 10° trim to the water surface. The moment arm of the resulting drag and lift forces from the planing surface should provide a righting moment sufficient to stabilize the craft at the roll or pitch angle from the plough-in.

4.7 Overturning in waves

Accidents of this type have occurred to ACVs as shown in Table 1.4. SR.N6–012, running on a passenger route between Portsmouth and Ryde, Isle of Wight, in England, overturned in March 1972, a result of the combined action of wind and waves. The craft flooded, which led to capsizing due to the waves and the deaths of five passengers.

This is the biggest tragedy in ACV/SES transport history to date. Figure 4.54 [51] describes the situation of the ACV at that time. Owing to the large winds and waves, the driver decided to navigate the craft along the beach. However, the surf close to the beach was very steep and acted with the wind and tide on the craft which had to run in beam seas and this caused the craft to roll severely, the side skirt to tuck under at the trough of a wave and then the craft capsized.

At that time the wind speed was about 60 knots, wave height 4.6 m, the speed of

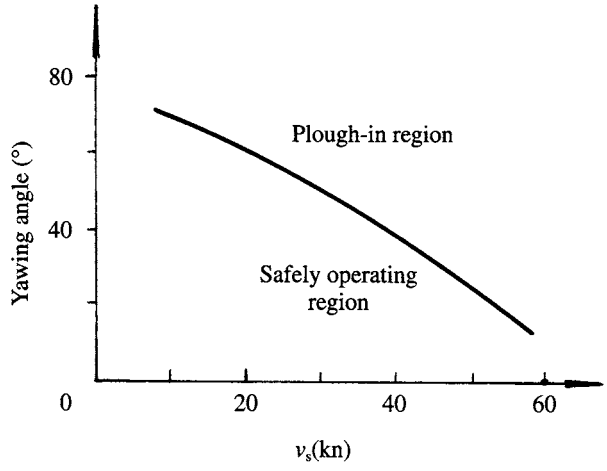

Fig. 4.53 The plough-in boundary of SR.N6.

circular motion of water particles 11 knots and speed of tide flow was about 4 knots. It is clear that part of the fault was due to incorrect craft navigation, but at least it teaches us a lesson that while it may seem safe to navigate a craft along the beach, as a matter of fact it is not safe due to the high surf which could act on the craft to capsize it in heavy weather.

Following this accident, the UK government set up an investigation, which included a major study of hovercraft stability including parametric model tests of several current large craft designs to identify possible improvements, particularly to the skirt systems [48]. This study produced much useful information and led to the development of the bulbous bow skirt, the tapered skirt and revised cushion feed designs. Some of these items have been introduced above, the remainder will be described in Chapter 7.

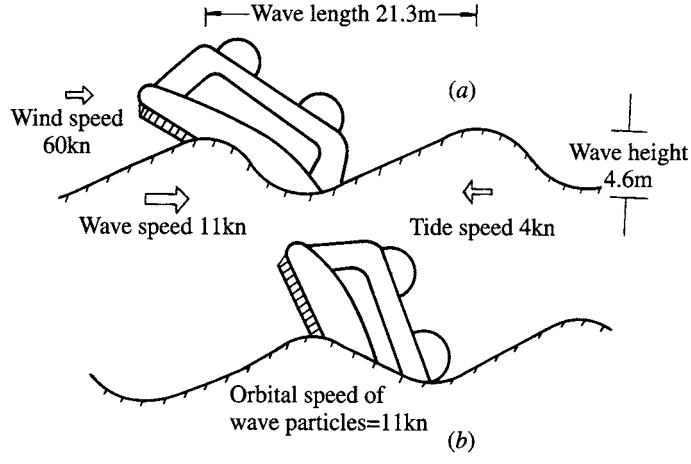

Fig. 4.54 The overturning of SR.N6 in very steep beam waves.